

# Geotechnical Engineering

## Understanding Rock-Steel interface properties for use in offshore applications

--Manuscript Draft--

<b>Manuscript Number:</b>	GE-D-20-00183R3
<b>Full Title:</b>	Understanding Rock-Steel interface properties for use in offshore applications
<b>Article Type:</b>	Paper
<b>Corresponding Author:</b>	Michael John Brown, BEng, PhD, GMICE University of Dundee Dundee, Scotland UNITED KINGDOM
<b>Corresponding Author Secondary Information:</b>	
<b>Corresponding Author's Institution:</b>	University of Dundee
<b>Corresponding Author's Secondary Institution:</b>	
<b>First Author:</b>	Andreas Ziogos, MEng, PhD, GMICE
<b>First Author Secondary Information:</b>	
<b>Order of Authors:</b>	Andreas Ziogos, MEng, PhD, GMICE Michael John Brown, BEng, PhD, GMICE Ana Ivanovic, MEng, PhD, CEng, MICE Neil Morgan, BEng PhD CEng IMarE
<b>Order of Authors Secondary Information:</b>	
<b>Abstract:</b>	<p>The properties of unbonded rock-steel interfaces and the characteristics that control this behaviour seems to be an under researched area in terms of geotechnical application for example in the design of gravity-based foundation systems or dead weight anchors and the interaction of pipelines on rock. Whilst basic guidance does exist for rock-rock interfaces or pipeline behaviour, this focuses on macro roughness with little consideration of micro roughness, relative roughness of the surfaces or their strengths and hardness. Therefore in order for design and understanding to develop in these areas there is a need for basic interface friction parameters and understanding of the interface characteristics that control the strength of the interface such that correct values can be used but also so that the interface properties can be best manipulated to improve interface interaction. This paper presents interface friction angles for four types of rock sheared against steel interfaces of different roughness at a variety of normal stresses. The rocks themselves have a range of surface roughness, strength and hardness. The results of the testing programme are used to improve a simple analytical approach for predicting the shear strength of rock-steel interfaces that allows input of key controlling parameters.</p>
<b>Additional Information:</b>	
<b>Question</b>	<b>Response</b>
Please enter the number of total words in your abstract, main text and references.	6300
Please enter the number of figures, photographs and tables in your submission.	Figures 10 Tables 5
<b>Funding Information:</b>	

1 Date of resubmission: 16/02/21  
2 Date of resubmission: 04/02/21  
3 Date of resubmission: 30/09/20  
4 Date of initial submission: 09/08/20  
5

6 Paper number: GE-D-20-00183R3  
7

8 Title: Understanding Rock-Steel interface properties for use in offshore applications  
9 Author list: Andreas Ziogos, Michael John Brown\*, Ana Ivanovic and Neil Morgan  
10

11 \*corresponding author  
12  
13

14 Authors:

15 Dr Andreas Ziogos, MEng PhD GMICE  
16 Project Manager, White Research, Avenue de al Toison d'Or 67, 1060, Brussels, Belgium  
17 ORCID: 0000-0002-4634-3506  
18 Email: aziogos@white-research.eu  
19  
20

21 \*Prof Michael John Brown, BEng PhD GMICE  
22 Professor, School of Science and Engineering, University of Dundee, Fulton Building, Dundee,  
23 Scotland, DD14HN, UK  
24 ORCID: 0000-0001-6770-4836  
25 Email: m.j.z.brown@dundee.ac.uk  
26  
27

28 Prof Ana Ivanovic, MEng PhD CEng MICE  
29 Professor, School of Engineering, University of Aberdeen, Fraser Noble Building, Aberdeen, Scotland,  
30 AB24 3FX, UK  
31 ORCID: 0000-0002-5437-2550  
32 Email: a.ivanovic@abdn.ac.uk  
33  
34

35 Dr Neil Morgan, BEng PhD CEng IMarE  
36 Principal Geotechnical Engineer, Lloyd's Register EMEA, Kingswells Causeway, Prime Four Business  
37 Park, Kingswells, Aberdeen, AB15 8PU  
38 ORCID: 0000-0002-5944-0188  
39 Email: neil.morgan@lr.org  
40  
41

42 Word count: 6603  
43 Number of figures: 13  
44 Number of tables: 5  
45  
46  
47  
48  
49  
50  
51  
52  
53  
54  
55  
56  
57  
58  
59  
60  
61  
62  
63  
64  
65

# Understanding Rock-Steel interface properties for use in offshore applications

Andreas Ziogos, Michael John Brown\*, Ana Ivanovic and Neil Morgan

## Abstract

The properties of unbonded rock-steel interfaces and the characteristics that control this behaviour seems to be an under researched area in terms of geotechnical application for example in the design of gravity-based foundation systems or dead weight anchors and the interaction of pipelines on rock. Whilst basic guidance does exist for rock-rock interfaces or pipeline behaviour, this focuses on macro roughness with little consideration of micro roughness, relative roughness of the surfaces or their strengths and hardness. Therefore in order for design and understanding to develop in these areas there is a need for basic interface friction parameters and understanding of the interface characteristics that control the strength of the interface such that correct values can be used but also so that the interface properties can be best manipulated to improve interface interaction. This paper presents interface friction angles for four types of rock sheared against steel interfaces of different roughness at a variety of normal stresses. The rocks themselves have a range of surface roughness, strength and hardness. The results of the testing programme are used to improve a simple analytical approach for predicting the shear strength of rock-steel interfaces that allows input of key controlling parameters.

**Keywords:** Geotechnical engineering, Strength & testing of materials, Foundations.

## Notation list

1		
2	b	fitting constant
3	c	fitting constant
4	CNS	constant normal stiffness
5	d	linear displacement
6	$D_{50}$	mean particle size of soil
7	GBS	gravity base structure
8	IST	interface shear tester
9	M	relative hardness ratio
10	$M_{,rock}$	Mohs relative hardness of rock
11	$M_{,steel}$	Mohs relative hardness of steel
12	R	roughness ratio
13	$R_a$	average centreline roughness
14	$R_{a,rock}$	average centreline roughness of rock interface
15	$R_{a,steel}$	average centreline roughness of steel interface
16	$R_{max}$	vertical distance between the highest peak and lowest valley of the steel surface profile
17	$R_n$	relative roughness ratio for granular materials
18	$R_p$	radial position in IST test
19	r	sample radius
20	T	torque
21	$T_0$	rock tensile strength
22	UCS	unconfined compressive strength
23	$\alpha$	normalised shear strength (Alpha factor)
24	$\delta$	interface friction angle
25	$\theta$	rotational displacement
26	$\mu$	coefficient of friction
27	$\phi_b$	basic friction angle
28	$\sigma_n$	normal stress
29	$\sigma_v$	vertical stress
30	$\tau$	shear stress
31		
32		
33		
34		
35		
36		
37		
38		
39		
40		
41		
42		
43		
44		
45		
46		
47		
48		
49		
50		
51		
52		
53		
54		
55		
56		
57		
58		
59		
60		
61		
62		
63		
64		
65		

## 1 Introduction

Interfaces between construction materials and rock exist in many geotechnical or rock mechanics applications but often these are bonded due to the use of cementitious materials. For example, at the interface between the base of a dam or cast in situ pile rock sockets (Horvath, 1978; Rosenberg and Journeaux, 1976; Williams and Pells, 1981, Ball et al., 2018) and rock–steel interfaces such as rock bolts (Li and Håkansson, 1999) or H-steel piles driven into rock (Yu et al., 2013). These rock–steel interface examples result in constant normal stiffness (CNS) conditions, which lead to high normal stresses where the interface is subject to shear and constraint of dilation. This can result in interface normal stresses that are much higher than in other applications such as lightweight gravity based foundations or dead weight anchors (tidal stream generator foundations, Ziogos et al., 2017, or anchoring for aquaculture) and subsea pipeline installation and operation (e.g. restraint to axial and lateral walking of pipelines, Griffiths et al., 2019). Previous examples are of concrete bonded to rock or dowelled rock-concrete interfaces and there is a dearth of information relevant to certain applications.

One of the few publications relevant to offshore application NAVFAC (1986) suggests a coefficient of friction,  $\mu$ , of 0.7 (interface friction angle,  $\delta= 35^\circ$ ) for mass concrete on clean, sound rock. However, the origins of this value are unclear, and it is not stated if this refers to a bonded or unbonded surface, or the types of rock. Investigation of soil-steel interfaces is more common, for example to aid understanding of pile shaft behaviour (Kishida and Uesugi, 1986, Jardine et al., 1993) where it was found that the behaviour of the interface is affected by the surface characteristics of both interface elements (i.e. shape and size of sand grains, roughness of steel etc.). Therefore, taking account of only the steel surface roughness is not appropriate and a relative roughness ratio was proposed ( $R_n = R_{max}/D_{50}$ , where  $R_{max}$  is the vertical distance between the highest peak and lowest valley of the steel surface profile and  $D_{50}$  is the mean particle size of the soil) to investigate the overall effect of the roughness. It might be assumed that greater guidance on rock-interface shearing behaviour could be found in the rock mechanics or engineering geology literature but interface behaviour in these disciplines normally focuses on rock-rock joint interaction (Barton and Choubey, 1977) or faults where relative block movement may occur and interfaces may be infilled with soil materials. Where rock-rock interfaces are investigated these are considered to be controlled by macro roughness or “waviness” (Griffiths et al., 2019) where roughness is measured in terms of centimetres or metres rather than micro metres (unit normally adopted for average centreline steel roughness measurements,  $R_a$ ).

A simplistic analytical approach for predicting the shear resistance of a rock-steel interfaces was previously outlined by Ziogos et al. (2015a) and Ziogos et al. (2017), referred to as an alpha factor approach which was originally derived from shear box testing of steel against grout interfaces (used as rock analogues where unconfined compressive strength, UCS can be varied for the grout, Ziogos, 2020). This has a similar form to the approach outlined in Tomlinson (2001) to predict the shear resistance of cast-in-situ pile rock sockets which recognises the rock strength (UCS) although only rock-steel interfaces at relative low normal stresses are considered here i.e. not those associated with pile driving.

$$\alpha = b \left( \frac{UCS}{\sigma_n} \right)^c \quad 1$$

Where  $\alpha = \frac{\tau}{UCS}$  equals the shear stress,  $\tau$  divided by the rock strength (UCS)

Equation 1 can be solved for shear stress ( $\tau$ ) leading to:

$$\tau = b \frac{UCS^{(c+1)}}{\sigma_n^c}$$

2

1  
2  
3 Where:  $\tau$  = shear stress, UCS = rock unconfined compressive strength,  $\sigma_n$  = normal stress and b and c  
4 = arithmetic constants.

5  
6 Although this approach captures the normal stress applied and the rock strength, it does not recognise  
7 the roughness or relative roughness of the interface materials and requires further development for  
8 rock rather than grout-steel interfaces.  
9

10 This paper outlines the results of rock-steel interface testing of various rock types from the United  
11 Kingdom considering the effects of normal stress, roughness of the interfaces, rock strength and the  
12 hardness of the surfaces. This is used to provide a useful database of material parameters for design  
13 and further develop a simplistic method for estimating rock-steel interface shear resistance.  
14  
15

## 16 **2. Laboratory testing**

### 17 **2.1 Description of rock samples used for laboratory testing**

18  
19 The rock samples were originally selected to reflect rock types at areas of tidal stream generation  
20 potential (Sandstone, Andesite and Flagstone) in Scotland where gravity based structures may be  
21 deployed (Ziogos et al., 2015b). It was then decided to broaden this to include Limestone, which is  
22 generally absent in Scotland, and Chalk (Ziogos et al., 2017), to align with the interest in deployment  
23 of wind energy foundations in the UK and Europe (Buckley et al., 2020). The Sandstone and Flagstone  
24 samples were sourced from the Caithness area of Scotland (North East), UK. The Sandstone came from  
25 Warth Hill disused quarry, south of John O’Groats, Scotland (National Grid coordinate: ND37150  
26 70138). The Old Red Sandstone was yellow-orange in colour and medium grained (Johnstone and  
27 Mykura, 1989) and described as medium strong. The Flagstone was obtained from an active Caithness  
28 Flagstone quarry (Devonian, Spital Flagstone formation) near Achscrabster (National Grid coordinate:  
29 ND07829 63333). Caithness Flagstones are laminated siltstones and mudstones (Geological Survey of  
30 Scotland, 1914). The samples collected were very strong fine grained and dark-grey in colour. The  
31 Limestone samples were obtained from the active Limestone quarry near Dunbar, East Lothian,  
32 Scotland, UK (National Grid coordinate: NT71668 76718). The Limestone was a very strong Middle  
33 Skateraw Limestone, a fine grained, grey coloured Carboniferous Limestone from the Lower  
34 Limestone Group (British Regional Geology, 1971). The Andesite samples were recovered from the  
35 active Ardownie quarry located 8 km north east of Dundee, Scotland, UK (National Grid coordinate:  
36 NO48752 33934). The quarry lies in the Devonian, igneous Ochil volcanic formation, and the Andesite  
37 consist of a fine grained, very strong dark grey coloured igneous rock (Armstrong et al., 1985). Further  
38 details on the sampling and local setting of the rock samples used to prepare the element tests can be  
39 found in Ziogos (2020). Images of the saw cut rock samples prepared for testing are shown in Figure  
40 1.  
41  
42  
43  
44  
45  
46  
47  
48

### 49 **2.2 Scope of testing**

50  
51 Interface testing between rock–steel interfaces at normal stresses relevant to those anticipated in real  
52 tidal stream projects (Ziogos et al., 2015b) had previously been used in order to obtain the friction  
53 properties necessary for the determination of the sliding resistance of a gravity based structure (GBS).  
54 The same level of normal stresses was used here. In addition, the effect of steel roughness was  
55 investigated ( $R_a$  = 0.4, 7.2 and 34  $\mu\text{m}$ , Table 1,  $R_a$  refers to centre-line average roughness, as outlined  
56 in section 2.6) along with the effect of normal stress ( $\sigma_v$  or  $\sigma_n$  = 16, 79, 159 and 316  $\text{kN/m}^2$ ) over  
57 displacements of 10 mm during shear. The range of steel roughness investigated covers the roughness  
58 of some of the steel elements commonly found in geotechnical applications (for example,  $R_a$  = 5–10  
59  
60  
61  
62  
63  
64  
65

1  $\mu\text{m}$  for steel piles, Barmpopoulos et al., 2010). Initially, tilt table testing of rock-rock interfaces was  
2 undertaken to define the rock-rock basic friction angle ( $\phi_b$ ) which is a common parameter in rock  
3 mechanics. This was followed by rock-steel interface testing to allow comparison of the interface  
4 measurement using this simplistic equipment with that of the more advanced IST testing (Interface  
5 shear tester, as introduced in section 2.4). This was then followed by the use of the IST to test rock-  
6 steel interfaces over a range of normal stresses. IST testing and tilt table testing were undertaken in  
7 parallel to see if the results of the low-cost tilt table could be used to derive useful interface  
8 characterisation without the requirement for more specialised equipment.  
9

### 10 **2.3 Tilt table testing**

11 Prior to the main interface testing the basic friction angle (rock-rock) of the rock samples (e.g.  
12 Sandstone,  $\phi_b = 30.5^\circ$ ) was determined using the tilt table test in line with the methodology outlined  
13 in USBR 6258 (USBR, 2009). This involves tilt table testing of two 54 mm diameter rock samples of 27  
14 mm thickness placed on top of each other (this size of sample was used for all testing). The samples  
15 were prepared by coring of a block of the sampled rock and then dry crosscutting of the core using a  
16 diamond saw. The interface frictional resistance was determined on this saw-cut surface (as per USBR  
17 6258) for all tilt table and IST testing. The  $\phi_b$  determined for the various rock types is summarised in  
18 Table 2. Previous results from the low normal stress tilt table tests show good correlation with the  
19 more advanced testing techniques at elevated stress levels (Ziogos et al., 2017, Ziogos, 2020). Apart  
20 from using the tilt table test to determine the basic friction angle, this simple test was also used to  
21 test the rock samples against the steel interfaces (Figure 2) to see how the more advanced testing  
22 compared with the basic tilt table test. All samples tested in this study were dry. The tilt table consisted  
23 of a Controls joint roughness coefficient test device (32-B0096) capable of inclination of up to 50  
24 degrees with a top surface plate of square area 265 mm by 170 mm.  
25  
26  
27  
28  
29  
30

### 31 **2.4 Description of the Interface shear tester (IST) device**

32 A computer-controlled torsional interface shear tester (IST, GDS Instruments, UK) was used for  
33 interface shear testing (Figure 3). This device consists of an axial actuator at the top of the rig, which  
34 can apply up to 5 kN of vertical load, and a rotational actuation system at the base, capable of applying  
35 torque up to 200 Nm. Below the axial actuator is a combined load/torque cell arrangement with  
36 capacities of 5 kN and 200 Nm, respectively. The axial actuator applies the normal load to the samples  
37 under test and is fixed against rotation, whereas the rotational actuator applies the torque/rotation  
38 from below. Images and a more detailed description of this equipment can be found in Ziogos et al.  
39 (2017) and Ziogos (2020).  
40  
41  
42  
43

44 A clamping system was developed to allow rectangular interchangeable steel interface elements of  
45 65x90 mm with a thickness of 8 mm to be clamped at the base of the rig above the rotational actuator.  
46 Similarly, below the load/torque load cell a clamping device was developed to clamp the rock samples.  
47 During the test, the upper rock sample was fixed while the lower steel sample rotated. During the  
48 tests torque and normal load were measured using the calibrated torque/load cell and vertical and  
49 rotational deformation measurements were automatically calculated by the counts of the stepper  
50 motor driving the low rotational actuation.  
51  
52  
53

54 The tests were conducted under constant normal stress conditions on dry samples under four  
55 different normal stress levels of 16, 79, 159, 316 kPa. The shearing rate was 0.005 mm/s of equivalent  
56 horizontal displacement. Each test was terminated at an equivalent horizontal displacement of 10 mm  
57 ( $42.5^\circ$  rotational displacement). The torque measured was converted to average shear stress as per  
58 Equation 3 after Saada and Townsend (1981) for ring shear testing.  
59  
60  
61  
62  
63  
64  
65

$$\tau = \frac{T}{\int_0^r 2\pi r^2 dR_p} = \frac{2}{2\pi r^3} T \quad 3$$

The radial deformation was converted to a linear displacement at a reference point considered at a distance equal to half of the radial length of the circular rock sample, as per Equation 4.

$$d = \theta \frac{r\pi}{360} \quad 4$$

where  $\theta$  is rotational displacement,  $\tau$  is shear stress,  $d$  is linear displacement,  $r$  is the rock sample radius,  $R_p$  is radial position and  $T$  is torque.

## 2.5 Description of steel interface samples

Mild steel (EN24T) was used to prepare the rectangular (65×95×8 mm) steel plates. As discussed in the introduction (Ziogos et al., 2015a, 2015b), roughness has a major effect on the interface behaviour, therefore different preparation techniques (polishing and machining) were applied and resulted in plates with a wide range of surface roughness ( $R_a$  between 0.4 and 34  $\mu\text{m}$ ). Polishing with a surface grinder using a BAA60 – K7V wheel resulted in surface roughness average  $R_a = 0.4 \mu\text{m}$ . Machining, using a shaping machine and an appropriately adjusted shaping tool, resulted in  $R_a$  values of 7.2 and 34  $\mu\text{m}$ .

## 2.6 Rock and steel characterisation

The Interface roughness parameter selected to reflect the rock and steel roughness was  $R_a$  (centre-line average roughness), which is the average of all deviations of the roughness profile from the median (centre) line over a defined profile length (Degarmo et al., 2003). A Taylor Hobson Surtronic Duo stylus contact profilometer was used to determine  $R_a$ . For each sample and interface, five  $R_a$  measurements were taken and the mean value was selected. The average interface properties of the materials used for testing (rock and steel samples) are summarised in Table 1 and 2. In line with similar approaches for sand-steel interfaces a relative roughness (R) approach was used in this study:

$$R = R_{a,steel}/R_{a,rock} \quad 5$$

Steel plates with  $R_a = 0.4, 7.2$  and  $34.0 \mu\text{m}$  were used, leading to values of roughness ratio (R) between 0.021 (rock significantly rougher than steel) and 12.592 (steel significantly rougher than rock).

The hardness of both the rock and steel interfaces (Table 3) was determined by the relative scratch test using hardness picks manufactured from different materials and hardness with each pick designed to reflect a particular Mohs hardness (between 2 to 9). The process of determining Mohs hardness is to attempt to scratch the surface of interest with a pick. The pick will either scratch the surface (if pick is harder than the surface), slide across it (indication of equal Mohs hardness) or leave behind a streak of the material of the pick (is softer than the surface). Based upon a trial and error process and varying the picks it is possible to determine an approximate material hardness. Although the methodology seems relatively simplistic the Mohs Hardness for the mild steel used is equal to 4 which converts to a Vickers Hardness of 315  $\text{kg}/\text{mm}^2$  (Vickers Hardness was not measured directly and is only given as an indicative value based upon conversion outlined in Petrescu, 1999). This is consistent with the manufacturer's upper hardness values specified for the mild steel (252-303  $\text{kg}/\text{mm}^2$ ).

Unconfined compression (direct method) to determine the unconfined compressive strength (UCS) normally consists of crushing rock cylinders. According to ISRM (2007), the cylinder should have height to diameter ratio equal to 2. For this research, 54 mm diameter samples were used, suggesting 108 mm high samples would be needed for standard UCS testing. Due to the inconvenient dimensions of the rock blocks retrieved from the field (not thick enough), cores appropriate for crushing in this



manner were only obtained from Sandstone samples. Thus, for the rest of the rock types, it was necessary to correlate the UCS to the tensile strength ( $T_0$ ) using the Brazilian test. Equation 6 was used to correlate tensile strength to UCS and was proposed by Altindag and Guney (2010), after analysing experimental data from various rock types.

$$UCS = 12.308T_0^{1.0725} \quad 6$$

Three tests per rock type were carried out and the mean value was used to calculate UCS. The results are summarised in Table 2.

### 3 Results and discussion

#### 3.1 Effects of surface roughness and normal stress

Typical data from IST testing is shown in Figure 4 for the Flagstone. A summary of all test data is provided in Table 4. The various interface combinations indicate a relatively similar response to that in Figure 4 with a slightly elevated initial shear stress (peak) followed by a reduction in shear stress post peak (or ultimate) and then remaining relatively constant until the end of the test. Typically, peak shear stress is observed at increasing displacement levels as normal stress increases though it is noted that peak shear stresses are reached at displacements typically less than 0.5mm suggesting that in-service design of such interfaces should be based upon ultimate rather than peak resistance. The data is generally rather “noisy” compared to conventional interface testing (sand – steel interfaces) due to the solid nature of the rock-interface. The asperities on a conventional steel surface apply stress to the grains of the sand during shearing resulting in displacement of the grains and the sand element is deformed (compliant interface). When two solid samples are sheared (i.e. steel and rock), the asperities of both elements of the interface are interacting, however the shear stress generated may not be adequate to cause significant deformation of the samples (i.e. non-compliant interface, especially under low normal stress levels). As a result, the shear stress generated fluctuates due to the surface topography of the elements.

Comparison of the relative behaviour of the different rock types against a steel interface with the same roughness for all rock types is shown in Figure 5. The Sandstone interface (the roughest of the rock types tested) exhibits the highest interface friction angle values ( $\delta$ ). Flagstone and Andesite have very similar  $R_a$  values (Table 4) and broadly similar interface friction behaviour albeit with lower friction angles for the Flagstone (Figure 5). Limestone is significantly smoother resulting in the weakest interface especially for smoothest steel interface ( $R_a = 0.4 \mu\text{m}$ ).

Figure 6 shows how the peak and ultimate interface friction angles of the various rock types tested against the steel interfaces varies with respect to applied normal stresses. The basic friction angle ( $\phi_b$ ) is also shown (rock-rock). In addition to the basic friction angle, the figure shows the range of tilt table results for the different steel surface roughness ( $R_a = 0.4$  and  $34 \mu\text{m}$ , rock-steel). The results are also annotated with the relative roughness ratio,  $R$ . Figure 6 shows that irrespective of the rock type, the interfaces typically exhibit the highest friction angle at the low normal stress of 16 kPa. The interface friction angle decreases with increasing normal stress up to 159 kPa and tends to a lower value between 159 and 316 kPa where little variation is noticed. This decrease of interface friction angle with increasing normal stress is in accordance with the findings of Abuel-Naga et al., (2018). They investigated the effect of the surface properties (roughness and hardness) of glass fibre reinforced polymer, copper, mild steel and high carbon steel on the shear behaviour of continuum – granular material interfaces and found that the interface friction angle reduced with increasing normal stress. They conducted interface shear box tests at normal stresses of 56, 97 and 184 kPa and a reduction of

up to 25% was observed when the normal stress increased from 56 to 184 kPa, however the mechanism was not discussed further.

Based on Figure 4, and also by comparing the peak and ultimate values for each individual rock – steel combination (Figure 6), it can be seen that all the interfaces exhibit a “brittle” type behaviour where in general the ultimate friction angles are significantly lower than the peak values (by over 50% in some cases). At low normal stress levels (16 kPa), peak interface friction angle values (Figure 6a, c, e, g) tend to the basic friction angle ( $\phi_b$ ) which is usually (apart from Limestone) higher than tilt table results for the rock – steel interface tests. Thus, this could be proposed as a method to determine the upper bound shear resistance using a simple tilt table and at low stress suggests the rock interface is dominating the interface behaviour. This though is not clear in the case of limestone. It would also appear that for the rougher rock samples (Sandstone and Andesite) that the tilt table testing could be used to bracket the complete behaviour (Figure 6a, b, e, f) over a range of rock-steel relative roughness.

When the smoothest steel interface is considered ( $R_a = 0.4 \mu\text{m}$ ), the roughness ratio ( $R$ ) values vary between 0.021 (Sandstone) and 0.148 (Limestone) (Table 1). The Sandstone which has the roughest surface ( $R_a = 19 \mu\text{m}$ ) – polished steel interface is the strongest (Figure 5), exhibiting  $\delta_{\text{peak}}$  between  $38^\circ$  and  $29^\circ$  (Figure 6a) and  $\delta_{\text{ultimate}}$  between  $29^\circ$  and  $24^\circ$  (Figure 6b) depending on the applied normal stress (Table 4). In the case of Flagstone ( $R_a = 5.5 \mu\text{m}$ ), the interface yields lower peak ( $\delta_{\text{peak}} = 33^\circ - 18^\circ$ ) and ultimate values ( $\delta_{\text{ultimate}} = 25^\circ - 13^\circ$ ) depending on normal stress (Figure 6c, d). Whereas, for Andesite ( $R_a = 5.8 \mu\text{m}$ ),  $\delta_{\text{peak}}$  ranges between  $27^\circ$  and  $25^\circ$  and  $\delta_{\text{ultimate}}$  is remarkably consistent around  $21^\circ$  irrespective of normal stress (Figure 6e, f). For Limestone ( $R_a = 2.7 \mu\text{m}$ ), which is the smoothest rock tested, the interface becomes significantly weaker, exhibiting  $\delta_{\text{peak}}$  between  $17^\circ$  and  $10^\circ$  and  $\delta_{\text{ultimate}}$  between  $13^\circ$  and  $7^\circ$  (Figure 6g, h). It would appear that these lower values are a result of very low surface roughness of both interacting materials (i.e. Limestone and steel,  $R=0.148$ ). The effect of relative roughness,  $R$ , is considered separately in Figure 7.

The average interface friction angle of the tests at 159 and 316 kPa (where the interface behaviour seems to be more consistent) is shown for each individual rock – steel combination (Figure 7). Although it might be expected that relative roughness,  $R$  may dominate behaviour it is apparent that the variation of  $R$  doesn't have the same effect on all the interfaces. Sandstone and Andesite don't appear to be significantly affected by  $R$  (over the range studied) whereas the interface friction angle for Flagstone and Limestone interfaces appear to increase significantly. This behaviour is different to that exhibited for continuum material – sand interfaces (Jardine et al., 1993, Abuel-Naga et al., 2018), where the upper limit of the interface shear strength is defined by the internal friction angle of the granular material where the solid interface becomes so rough that it effectively grabs soil particles and induces full soil-soil shear. The apparent variation of the effect of  $R$  suggests that although roughness influences, other interface properties are also having an effect.

### 3.2 Considering surface hardness

To further investigate this behaviour, it was decided to consider interface relative hardness (Table 3, Equation 7). This is not something a geotechnical engineer dealing with soil-structure interfaces would normally consider due to the relative stiffness of construction material where soil deformation would normally occur well before any interface damage. The relative scratch hardness has been identified in the literature as a factor that affects the shear deformation of continuum – continuum (Engelder and Scholz, 1976) and continuum – granular material interfaces (Abuel-Naga et al., 2018). When one of the two counter faces is harder, then ploughing occurs (harder surface into the softer surface) during shear (Engelder and Scholz, 1976). In this study, a relative hardness ratio  $M$  has been defined:

$$M = Mohs_{steel}/Mohs_{rock}$$

1  
2 The Mohs hardness value for the Sandstone is 7, for Andesite 6 (Table 3) and for the steel 4, resulting  
3 in M values of 0.57 and 0.67 for Sandstone and Andesite interfaces respectively (i.e. the rock is harder  
4 than the steel). This suggests that no ploughing of the steel into the rock surface occurs, although rock  
5 asperities could plough into the steel surface. This also explains the consistency between the  
6 behaviour in these two rock types (Figure 7) where the rocks have similar hardness and plough into  
7 the steel, which although had different roughness between tests, was fabricated consistently from  
8 Grade EN24T steel. Thus, in this case (Sandstone and Andesite) the steel interface is the one that may  
9 be more influential in terms of variability or relative behaviour than the rock. As seen in Figure 6a and  
10 3e the peak interface friction angle values are higher for low normal stresses (up to 79 kPa) and  
11 increase with increasing steel roughness. As normal stress increases (159 and 316 kPa), peak interface  
12 friction angles reduce, and the effect of steel roughness becomes less apparent (Figure 7). This  
13 suggests that as the stress increases there is an increase in ploughing occurring into the steel and at  
14 low stress the asperities of the rock are riding over the peaks in roughness of the steel with limited  
15 damage to either surface. This is supported by measurement of small deflections that occur between  
16 the platens of the IST interfaces (Figure 8). The displacement is dilatant (positive) for normal stress of  
17 16 kPa and contractive (negative) for normal stress of 316 kPa. In addition, dilation seems to be greater  
18 for increasing steel  $R_a$  and roughness ratio R (at normal stress of 16kPa), whereas at normal stress of  
19 316 kPa the contraction is similar irrespective of steel roughness thus roughness plays a greater role  
20 at lower stress.  
21

22  
23  
24  
25  
26  
27 Ultimate friction angle observations also support this assumption in that the effect of both normal  
28 stress and steel  $R_a$  is rather minimal at larger strains or displacements as can be seen in Figure 6b and  
29 Figure 6f. Therefore, once the initial low stress dilation has occurred or the surface has been damaged  
30 the shearing behaviour on the interface for the harder Sandstone and Andesite becomes independent  
31 of the initial surface steel roughness or normal stress. The tilt table tests using steel  $R_a = 0.4 \mu\text{m}$  lie  
32 below the lower values observed from IST testing (typically for steel  $R_a = 0.4 \mu\text{m}$ ) as far as peak and  
33 ultimate values are concerned (Figure 6a, b, e, f). Thus, tilt table test of the smoother interfaces seems  
34 to be able to provide a lower bound value for Sandstone – steel and Andesite – steel interfaces at  
35 higher stresses. Whereas at lower stresses the basic friction angle could be used to estimate upper  
36 bound resistances especially for the rougher interfaces.  
37  
38  
39

40  
41 Considering the Flagstone – steel and Limestone – steel interfaces as exhibiting similar behaviour to  
42 each other, albeit Flagstone interfaces yield higher interface friction angles, both rock types have a  
43 Mohs hardness value similar to that of mild steel (Table 3). Limestone has a value of 4.5 and Flagstone  
44 has a value of 3 on the Mohs scale (Limestone is slightly harder, and Flagstone is softer). The interfaces  
45 exhibit the highest  $\delta$  peak values for  $\sigma_n = 16 \text{ kPa}$  because dilation is taking place and consequently  $\delta$   
46 peak increases with increasing steel  $R_a$  (Figure 6c, 6g and Figure 8b). As  $\sigma_n$  increases (159 and 316 kPa),  
47 dilation is suppressed (Figure 8a) however the effect of steel  $R_a$  is still apparent ( $\delta_{\text{peak}}$  is higher for steel  
48  $R_a = 34 \mu\text{m}$ ) in contrast to what was shown before for Sandstone and Andesite interfaces (Figure 8a).  
49 This happens because Flagstone and Limestone exhibit hardness values very close to that of the steel  
50 element. Therefore, it is believed that higher localised normal stress at the point of contact is required  
51 for ploughing to occur. As the normal stress increases, ploughing of the steel asperities into the rock  
52 surface (or vice versa depending on which material is harder) takes place during shearing. It is also  
53 apparent, that contraction (i.e. indicating ploughing) for Sandstone and Andesite interfaces is almost  
54 double that observed for Flagstone and Limestone interfaces (Figure 8b). This behaviour is in  
55 accordance with Engelder (1978), who showed that the mode of shearing depends on the applied  
56 normal stress and the hardness of the counter face materials. This phenomenon is more pronounced  
57  
58  
59  
60  
61  
62  
63  
64  
65

1 as steel  $R_a$  increases (for a given  $\sigma_n$ ), because actual applied normal stress at the contact points is  
2 potentially much higher compared to the nominal  $\sigma_n$  which is calculated as an average value (i.e. the  
3 applied normal force divide by the plan area of the rock surface). This seems to affect both the peak  
4 and ultimate interface friction angles. As shown in Figure 6c the tilt table test provides a lower bound  
5 value of peak shear resistance for the Flagstone – steel interfaces, irrespective of steel  $R_a$ . The tilt table  
6 tests seem to overestimate the ultimate values of shear resistance for steel  $R_a = 0.4$  and  $7.4 \mu\text{m}$ , thus  
7 a lower bound value can only be provided fo the steel  $R_a = 34 \mu\text{m}$  results when the ultimate values are  
8 considered (Figure 6d). The tilt table seems to overestimate the interface friction angles for the  
9 Limestone – steel interfaces irrespective of the steel roughness, with only the peak interface  
10 behaviour showing any correlation at lower stresses to the basic friction angle or that for the roughest  
11 steel.  
12  
13

14 The effect of relative Mohs Hardness on the test results are summarised in Figure 6a and b. Each figure  
15 contains three interface friction angle values per rock type (one per steel  $R_a$ ) and a line that groups  
16 the data points for each steel  $R_a$  value. As shown previously (Figure 6a to 6h),  $\delta$  varies significantly  
17 between 16 and 159 kPa, whereas it seems to settle between 159 and 316 kPa. Therefore, the average  
18 value of  $\delta$  from the tests at 159 and 316 kPa normal stress are considered in Figure 9.  
19  
20

21 Sandstone – steel interfaces ( $M = 0.57$ ) exhibit the highest values of interface friction and Limestone  
22 – steel interfaces ( $M = 0.89$ ) exhibit the lowest values. For steel  $R_a = 0.4$  and  $7.2 \mu\text{m}$ , interface friction  
23 angle values drop significantly between  $M = 0.57$  and  $M = 0.89$  and then delta increases again for  $M =$   
24  $1.33$  (Flagstone – steel). For steel  $R_a = 34 \mu\text{m}$  a similar pattern is followed, where the Limestone – steel  
25 interface again exhibits the lower values of  $\delta$ , although the difference to the  $\delta$  values of Andesite –  
26 steel and Flagstone – steel interfaces is not as significant as for steel  $R_a = 0.4$  and  $7.2 \mu\text{m}$ . In other  
27 words, it seems that the interface shear strength exhibits the lowest value when  $M$  is close to 1,  
28 whereas it increases as  $M$  displays values significantly different to 1 (i.e. where the rock interface is  
29 much harder or weaker than the steel). The Mohs hardness ratio  $M$  gives values close to 1, when the  
30 hardness of the steel and the rock are similar (e.g. 0.89 for Limestone – steel). In this case, it is believed  
31 that ploughing (of the harder material into the softer) is reduced during shearing (tending to sliding  
32 behaviour), thus leading to lower  $\delta$  values. This is supported by the reduced contraction seen in Figure  
33 8b. As the steel roughness increases, the localised stress at the points of contact is higher (fewer  
34 contact points) and ploughing becomes more apparent (i.e.  $\delta$  is similar for all rock types for the  
35 roughest steel interface and the effect of roughness is more important). If the rock is significantly  
36 harder than the steel, then ploughing of the rock into the steel takes place even under lower normal  
37 stress levels, leading to an increase in the interface shear strength. In a similar manner, when the steel  
38 is significantly harder than the rock, ploughing (scratching) of the steel into the rock takes place.  
39 However, taking into account the data in Figure 9, it is believed that  $\delta$  is higher when  $M$  tends to 0.5  
40 (i.e. rock harder than the steel), because steel is more ductile than rock. Therefore, it is felt that more  
41 energy is dissipated when rock ploughs (causing scratches) into the steel compared to when the steel  
42 ploughs into the rock surface. In terms of design optimisation this would suggest that it doesn't matter  
43 how hard the steel is if it is rough enough but where the steel is relatively smooth then it should ideally  
44 be softer than the rock.  
45  
46  
47  
48  
49  
50  
51  
52

### 53 **3.3 Analytical approach to determine shear resistance of rock-steel interfaces**

54 The results of this study are shown in Figures 10 as per the previous proposed alpha method as  
55 outlined in Equation 1 and 2. Contours have been plotted for the  $\alpha$  values of all the rock types for each  
56 value of steel  $R_a$  (i.e. 3 contours) and the fitting constants  $b$ ,  $c$  for each contour are listed in Table 5.  
57  
58  
59  
60  
61  
62  
63  
64  
65

Equation 2 can be used to estimate the shear strength of a steel interface in the field. Arithmetic constants  $b$  and  $c$  can be selected in a simple fashion to reflect the roughness of the final steel interface or to select an appropriate roughness if the surface can take additional preparation (i.e. roughened). It is suggested that this equation is used only for the range of UCS, roughness and normal stress used to derive it. In order to improve the parameter selection process, it was decided to fix  $c$  to -1.08 for peak and -1.14 for ultimate values and the regression process was repeated to determine  $b$ . The fitting parameter  $b$  is shown in terms of relative roughness,  $R$  in Figure 11. It can be seen that for  $R$  values of up to approximately 3, the data seems to have a parabolic shape whereas for values between 6 and 13 a linear pattern is observed. As described earlier, Sandstone - steel and Andesite - steel interfaces seem to exhibit similar behaviour, possibly due to the similar Mohs hardness value (and consequently  $M$ ). For the same reason, Flagstone - steel and Limestone - steel interfaces also exhibit similar behaviour. Therefore, it was decided to investigate the variation of  $b$  with  $R$ , for these two groups of rocks, individually (Figure 12).

The variation of arithmetic fitting constant  $b$  is represented by Equation 8 and 9 for peak and ultimate values, respectively for the Sandstone - steel and Andesite - steel interfaces:

$$b_{peak} = 0.857 - (0.00082R) \quad 8$$

$$b_{ultimate} = 0.968 + (0.00537R) \quad 9$$

Between  $R = 0.021$  and  $R = 5.862$ ,  $b_{peak}$  and  $b_{ultimate}$  values vary by only 0.5 % and 3.2 % respectively. This trend denotes a relatively minimal effect of  $R$  on arithmetic fitting constant  $b$ . Especially for peak values, the value of  $b$  seems to be unaffected by  $R$  and  $R$  could potentially be ignored in this case. For Flagstone and Limestone interfaces the relative roughness ratio ranges between 0.073 and 12.593. The variation of  $b$  within this range is described by Equation 10 and Equation 11.

$$b_{peak} = 0.494 + (0.03202R) \quad 10$$

$$b_{ultimate} = 0.468 + (0.04279R) \quad 11$$

The average  $b_{peak}$  and  $b_{ultimate}$  values vary by 80 % and 113 % respectively, exhibiting a significant effect of relative roughness ratio  $R$ , on the value of  $b$  and consequently the shear strength of the interface. This difference is explained by the relative hardness ratio of the interfaces, as discussed previously.

If the rock type of interest is the same as one of the aforementioned rock types (e.g. Old Red Sandstone, Flagstone etc), then the equations above can be used. If a different rock type is of interest the relative roughness can be determined and the selection of the appropriate  $b$  value can be based on the relative hardness ratio  $M$  of the interface. Equation 8 and 9 can be used for  $0.57 \leq M \leq 0.67$ . Equation 10 and 11 shall be used for  $0.89 \leq M \leq 1.33$ . However, it is believed that Equation 10 and 11 could also be used (conservatively since these equations will typically lead to lower values of  $b$  compared to Equation 8 and 9) for  $M$  values between 0.67 and 0.89. The relative hardness,  $M$  can take values between 0.4 and 4.0 (considering steel Mohs hardness = 4), however the aforementioned equations shall not be used for relative hardness  $M$  values outside of this range without additional testing.

Figure 13 shows that the approach performs relatively well when used to predict the interface friction angles of the four rock types across all roughness values when the input data is re-analysed. This should be the case as the input data to develop the refined analytical approach is the same as that shown here as measured. Figure 13a does show though the difficulty of applying the approach down at low stress levels and this would suggest that the approach should be reserved for higher stress levels only (Figure 13b), although the approach at lower stress levels appears generally conservative.

1 The results of this study highlight that rock-steel interface behaviour needs to capture several factors  
2 such as UCS, normal stress, relative roughness ratio, R and relative hardness ratio, M. It should be  
3 noted here that a harder rock doesn't necessarily have higher UCS. For example, Sandstone consists  
4 of hard silica grains, but the matrix is relatively weak leading to a lower UCS value compared to a  
5 "softer" rock that may have a high UCS (e.g. Flagstone). Thus, basing Interface strength on UCS alone  
6 is not appropriate. It is also apparent that there is scope for using different materials at the interfaces  
7 between a foundation and rock to try and take advantage of the observe ploughing effects. For  
8 example, a facing of high-density plastic or more sustainable wood could attached to a steel  
9 foundation element to encourage such behaviour. Where steel is used there may be scope for  
10 selecting the hardness of a particular type relative to that of the rock as apart from hardness, only the  
11 roughness of the steel can be modified. In the harder rock it would appear that relative hardness is a  
12 more important consideration than relative roughness. Whereas when the steel and rock have similar  
13 hardness there is a benefit in increasing the surface roughness of the steel.  
14  
15  
16

#### 17 **4 Summary and Conclusions**

18  
19 There is a dearth of information with respect to the behaviour of rock-steel interfaces where these  
20 are unbonded and at relatively low stresses. Interface characterisation information is particular useful  
21 for lightweight gravity structures placed upon a rock seabed or the behaviour of pipelines laid on the  
22 seabed. This study has attempted to develop a basic data set to improve this lack of existing  
23 information for a limited range of rock types found across the UK. As well as presenting useful design  
24 input parameters the study has also investigated the effect of various controlling rock/interface  
25 characteristics on the interface strength. This has included the roughness or relative roughness, the  
26 rock strength (UCS) and the relative hardness of the interface surfaces.  
27  
28  
29

30 The results show that as in soil interfaces the normal stress has significant control on the strength of  
31 the interface, but this influence is non-linear with larger friction angles obtained at low stresses due  
32 to dilation and the interface asperities riding over each other as indicated by small upward movements  
33 on the interface. At higher stress levels friction angles reduce and the shearing behaviour becomes  
34 less erratic. Due to the nature of the interfaces, peak shear resistance occurs at relatively low  
35 displacements so it is suggested that it is more appropriate to use ultimate friction angles in design.  
36  
37

38 It is important for such solid interfaces that the hardness and relative hardness is given due  
39 consideration, and that this may control behaviour rather than just purely relative surface roughness.  
40 Where the hardness of the two counter faces (rock and steel) differs significantly (e.g. Sandstone and  
41 Andesite), the shearing consists of ploughing (irrespective of steel  $R_a$ ) and the interfaces exhibit similar  
42 behaviour. In contrast, Flagstone and Limestone interfaces have relative hardness ratio M close to 1  
43 (i.e. the rock surface has similar hardness to the steel interface). As a result, higher localised stress is  
44 required for ploughing to occur, hence the interfaces are affected more by the roughness of the steel.  
45 Increasing steel roughness, tends to increase the interface shear strength, however this is more  
46 apparent for M closer to 1 (i.e. Flagstone and Limestone). When M is significantly different to 1 (i.e.  
47 Sandstone and Andesite), the effect of steel roughness is minimised increases and ploughing into the  
48 steel (or into the rock) occurs.  
49  
50  
51  
52

53 A previously developed analytical approach to predicting the shear resistance on the interfaces  
54 (referred to as the alpha factor approach) was further improved to capture the behaviour of rock –  
55 steel interfaces and estimate the shear strength of interfaces within the UCS and normal stress range  
56 used in this study. This approach incorporates rock strength (UCS), normal stress on the interface,  
57 roughness and hardness to improve the prediction of the shear resistance of unbonded rock-steel  
58 interfaces. It is noted though that although this was developed based upon grout-steel interfaces and  
59  
60  
61  
62  
63  
64  
65

improved based upon the rock types investigated here, there is still a need for wider validation of this approach for different rock types and foundation interface materials outside of those tested here.

### Acknowledgements

The Energy Technology Partnership (ETP) and Lloyd's Register EMEA are gratefully acknowledged for the funding of this project. The authors would also like to acknowledge the support of the European Regional Development Fund (ERDF) SMART Centre at the University of Dundee that allowed purchase of the equipment used during this study. The views expressed are those of the authors alone, and do not necessarily represent the views of their respective companies or employing organisations.

### References

Abuel-Naga H M, Shaia H A and Bouazza A (2018) Effect of Surface Roughness and Hardness of Continuum Materials on Interface Shear Strength of Granular Materials. *Journal of Testing and Evaluation*, Vol. 46, No. 2, 2018, pp. 826–831, <https://doi.org/10.1520/JTE20160375>.

Altindag, R. & Guney, A. (2010). Predicting the Relationships between Brittleness and Mechanical Properties (UCS, TS and SH) of Rocks. In: *Scientific Research and Essays* Vol. 5(16), pp. 2107 – 2118.

Armstrong, M, Paterson IB and Browne MAE (1985) *Geology of the Perth and Dundee district*. British Geological Survey.

Ball J, Oram C, Hull, J and Hill J (2018) Maintained load-test results for continuous flight auger piles in south-east England Chalk. *Proc. of the Inst. of Civil Engineers: Geotechnical Engineering*, Vol 171, GE6, pp. 502-507.

Barmpopoulos IH, Ho TYK, Jardine RJ and Anh-Minh N (2010) The large displacement shear characteristics of granular media against concrete and steel interfaces. In *Characterization and Behavior of Interfaces*. Proceedings of the Research Symposium on Characterization and Behavior of Interfaces, Atlanta, Georgia, USA (Frost JD (ed.)).

Barton, N.R. & Choubey, V. (1977). The shear strength of rock fractures in theory and practice. *Rock Mechanics*, Vol. 10, pp. 1-54.

British Regional Geology (1971). *The South of Scotland*. Her Majesty's Stationery Office, Edinburgh.

Buckley RM, Jardine RJ, Kontoe S, Barbosa P and Schroede, SP (2020). Full-scale observations of dynamic and static axial responses of offshore piles driven in chalk and tills. *Géotechnique* 70, No. 8, 657–681, <https://doi.org/10.1680/jgeot.19.TI.001>.

Degarmo E, Black J and Kohser R (2003) *Materials and Processes in Manufacturing*, 9th ed. Wiley, Hoboken, NJ, USA.

Engelder, JT. (1978) Aspects of Asperity-Surface Interaction and Surface Damage of Rocks during Experimental Frictional Sliding. *Pure and Applied Geophysics* ,116: 705-716

Engelder JT and Scholz CH (1976) The role of asperity indentation and ploughing in rock friction, 2: Influence of relative hardness and normal load, *International Journal of Rock Mechanics and Mining Science*. 13, 155-163.

Geological Survey of Scotland. (1914). *The geology of Caithness*, printed under the authority of His Majesty's Stationery Office, 1914.

1 Griffiths T, White D, Draper S, Leighton A, Cheng L, An H and Fogliani A (2019) Lateral resistance of  
2 "rigid" pipelines and cables on rocky seabeds. Canadian Geotechnical Journal, 56 (6), 823-839.  
3 doi:10.1139/cgj-2018-0208.

4 Horvath RG (1978) Field load test data on concrete to rock bond strength for drilled pier foundation.  
5 University of Toronto, Toronto, Canada, Publication 78-07.

6  
7 ISRM (International Society for Rock Mechanics) (2007) The Blue Book. The Complete ISRM Suggested  
8 Methods for Rock Characterization, Testing and Monitoring: 1974–2006. ISRM, Lisbon, Portugal.

9  
10 Jardine RJ, Lehane BM and Everton SJ (1993) Friction coefficients for piles in sands and silts. Offshore  
11 Site Investigation and Foundation Behaviour Advances in Underwater Technology, Ocean Science and  
12 Offshore Engineering SUT, London, UK, vol. 28, pp. 661–677.

13  
14  
15 Johnstone GS and Mykura W (1989) British Regional Geology, The Northern Highlands of Scotland.  
16 British Geological Survey, Keyworth, Nottingham, UK.

17  
18 Kishida H and Uesugi M (1987) Tests of interface between sand and steel in the simple shear  
19 apparatus. Géotechnique 37(1): 45–52.

20  
21  
22 Li C and Håkansson U (1999) Performance of the Swellex bolt in hard and soft rocks. In Rock Support  
23 and Reinforcement Practice in Mining: Proceedings of the International Symposium on Ground  
24 Support (Villaescusa E, Windsor CR and Thompson AG (eds)). Balkema Publishers, Rotterdam, the  
25 Netherlands, pp. 103–108.

26  
27 Petrescu MI (1999) Self consistency between the Mohs hardness and the Vickers microhardness for  
28 some sulphides and sulphosalts. UPB Scientific Bulletin, Series B: Chemistry and Materials Science  
29 61(3-4):145-151.

30  
31  
32 Rosenberg P and Journeaux NL (1976) Friction and end bearing tests on bedrock for high capacity  
33 socket design. Canadian Geotechnical Journal 13(3): 324–333.

34  
35 Saada AS and Townsend FC (1981) State of the art: laboratory strength testing of soils. In Laboratory  
36 Shear Strength of Soil. (Young RN and Townsend FC (eds)). ASTM International, West Conshohocken,  
37 PA, USA, ASTM STP 740, pp. 7–77.

38  
39 Tomlinson MJ (2001) Foundation Design and Constructions, 7th edn. Pearson Education Limited,  
40 Harlow, UK.

41  
42  
43 Williams FP and Pells JN (1981) Side resistance rock sockets in sandstone, mudstone, and shale.  
44 Canadian Geotechnical Journal 18(4): 502–513.

45  
46 Uesugi M and Kishida H (1986) Influential factors of friction between steel and dry sand. Soils and  
47 Foundations 26(2): 33–46.

48  
49 USBR (United States Bureau of Reclamation) (2009) USBR 6258: Procedure for Determining the Angle  
50 of Basic Friction (Static) Using a Tilting Table Test. U.S. Department of the Interior Bureau of  
51 Reclamation, Technical Service Centre, Denver, CO, USA.

52  
53  
54 Yu ZX, Tham LG, Lee PKK, Liu YT and Wong MK (2013) A study on socketed steel H-piles under vertical  
55 load. HKIE Transactions 20(3): 172–187.

56  
57  
58 Ziogos A (2020) Investigation of the interface shearing resistance of steel and concrete on different  
59 rocks for renewable energy gravity foundation applications. PhD thesis. University of Dundee, UK.

60  
61  
62  
63  
64  
65



1 Ziogos A, Brown MJ, Ivanovic A and Morgan N (2015a) Investigation of rock-steel interface testing for  
2 gravity foundations for marine energy generators. In V. Meyer (eds) 3rd Int. Symp. on Frontiers in  
3 Offshore Geotechnics. Oslo, Norway. 10 -12 June 2015. Taylor & Francis Group, London. pp. 1245-  
4 1250.

5 Ziogos A, Brown MJ, Ivanovic A and Morgan N (2015b) Interface shear characteristics of Scottish rock  
6 samples from sites with tidal energy potential. XVI European Conference on Soil Mechanics and  
7 Geotechnical Engineering. 13 - 17 September 2015, Edinburgh, UK. ICE Publishing, London. pp. 1357-  
8 1362, DOI:10.1680/ecsmge.60678.

9 Ziogos A, Brown MJ, Ivanovic A and Morgan N (2017) Chalk-steel Interface testing for marine energy  
10 foundations. Proc. Inst. of Civil Engineers: Geotechnical Engineering Journal, Vol 170, GE3. pp. 285-  
11 298. DOI: 10.1680/jgeen.16.00112.

**Table caption list**

- 1
- 2 Table 1 Steel interface roughness values compared to those of the rock samples
- 3
- 4 Table 2 Summary of the rock characterisation parameters
- 5
- 6 Table 3 Summary of material surface hardness values
- 7
- 8 Table 4 Summary of results from rock – steel interface testing
- 9
- 10 Table 5 Summary of the arithmetic fitting constants b and c in Equation 1
- 11
- 12
- 13
- 14
- 15
- 16
- 17
- 18
- 19
- 20
- 21
- 22
- 23
- 24
- 25
- 26
- 27
- 28
- 29
- 30
- 31
- 32
- 33
- 34
- 35
- 36
- 37
- 38
- 39
- 40
- 41
- 42
- 43
- 44
- 45
- 46
- 47
- 48
- 49
- 50
- 51
- 52
- 53
- 54
- 55
- 56
- 57
- 58
- 59
- 60
- 61
- 62
- 63
- 64
- 65

## Figure caption list

1  
2 Figure 1 Images of the four rock types after saw cut preparation for interface shear testing a,  
3 sandstone, b, flagstone, c, andesite and d, limestone  
4

5 Figure 2 Image of the tilt table testing showing a sandstone sample on a steel interface during  
6 interface friction angle determination.  
7

8 Figure 3 a) Interface shear tester apparatus. b) Detailed view of the IST sample mounting  
9 arrangement.  
10

11 Figure 4 Results of IST testing Flagstone against a steel interface of  $R_a = 7.2 \mu\text{m}$   
12

13 Figure 5 Comparison of peak interface shear resistance for the different rock types tested against the  
14 smoothest steel interface at varying stress levels (steel interface  $R_a = 0.4 \mu\text{m}$ )  
15

16 Figure 6 Variation of peak and ultimate interface friction angles with normal stress for all of the rock  
17 types showing comparison of IST testing with results of tilt table tests  
18

19 Figure 7 The effect of relative roughness on the average interface friction angles at normal stresses  
20 of 159 and 361 kPa a) average peak interface friction angles, b) average ultimate interface friction  
21 angles  
22

23 Figure 8 Measurements of normal displacement during interface shear testing a) Sandstone and  
24 Andesite against steel of  $R_a = 0.4$  and  $34\mu\text{m}$ , b) Flagstone and Limestone against steel of  $R_a = 0.4$  and  
25  $34\mu\text{m}$   
26

27 Figure 9 Effect of relative hardness on the interface friction angle a) Average peak values of tests at  
28 159 and 316 kPa, b) Average ultimate values of tests at 159 and 316 kPa  
29

30 Figure 10 Alpha factor approach for predicting interface shear resistance showing contours for  
31 different steel roughness and corresponding arithmetic fitting constants  
32

33 Figure 11 Variation in arithmetic fitting constant  $b$  over the range of relative roughness investigated  
34

35 Figure 12 Variation of arithmetic fitting constant  $b_{\text{ultimate}}$  over a specific relative roughness range a)  
36 Relative roughness range for Sandstone and Andesite interfaces, b) Relative roughness range for  
37 Flagstone and Limestone interfaces  
38

39 Figure 13 Comparison of measured and calculated interface friction angles a) Test data at all normal  
40 stress levels tested (16 to 316 kPa, peak values), b) Test data from tests at normal stresses of 159  
41 and 316 kPa (peak values)  
42

# Journal Publishing Agreement

It is our policy to ask authors to assign the copyright of articles accepted for publication to the Publisher. Exceptions are possible for reasons of national rules or funding. Please tick the relevant options below.

In assigning copyright to us, you retain all proprietary rights including patent rights, and the right to make personal (non-commercial) use of the article, subject to acknowledgement of the journal as the original source of publication.

By signing this agreement, you are confirming that you have obtained permission from any co-authors and advised them of this copyright transfer. Kindly note that copyright transfer is not applicable to authors who are opting to publish their papers as Open Access. Open Access authors retain copyright of their published paper.

Please complete the form below and include it when you submit your article online (list of websites <http://www.icevirtuallibrary.com/page/authors/submitting-your-article>).

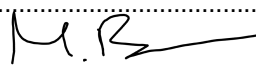
Journal name: ICE Geotechnical Engineering

Article title: Understanding rock-steel interface properties for use in offshore applications

Manuscript reference number: GE-D-20-00183

Authors: Ziogos, A, Brown, M.J, Ivanovic, A. & Morgan, N.

Your name: Michael Brown

Signature and date: 30/09/20 

Please tick either one option from part A or one option from part B. Please complete part C.

## A. Copyright

- I hereby assign and transfer the copyright of this paper to Thomas Telford Ltd.
- British Crown Copyright: I hereby assign a non-exclusive licence to publish to Thomas Telford Ltd.
- I am a US Government employee: employed by (name of agency) .....
- I am subject to the national rules of (country) ..... and confirm that I meet their requirements for copyright transfer or reproduction (please delete as appropriate)

## B. Authors with open access funding requirements. Please specify the Creative Commons license version required.

- CC-BY (for full details click here [Creative Commons Attribution \(CC BY\) 4.0 International License](https://creativecommons.org/licenses/by/4.0/))

## C. Please confirm that you have obtained permission from the original copyright holder. For ICE Publishing's copyright policy, please click [here](#). ICE Publishing is a signatory to the [STM Guidelines](#).

- I have obtained permission from the original copyright holder for the use of all subsidiary material included in this paper (E.g. for borrowed figures or tables).

**Response to reviewers**

Notation list added as required

Figure 1 Images of the four rock types after saw cut preparation for interface shear testing a, sandstone, b, flagstone, c, andesite and d, limestone

[Click here to access/download;Figure;Figure 1.jpg](#)

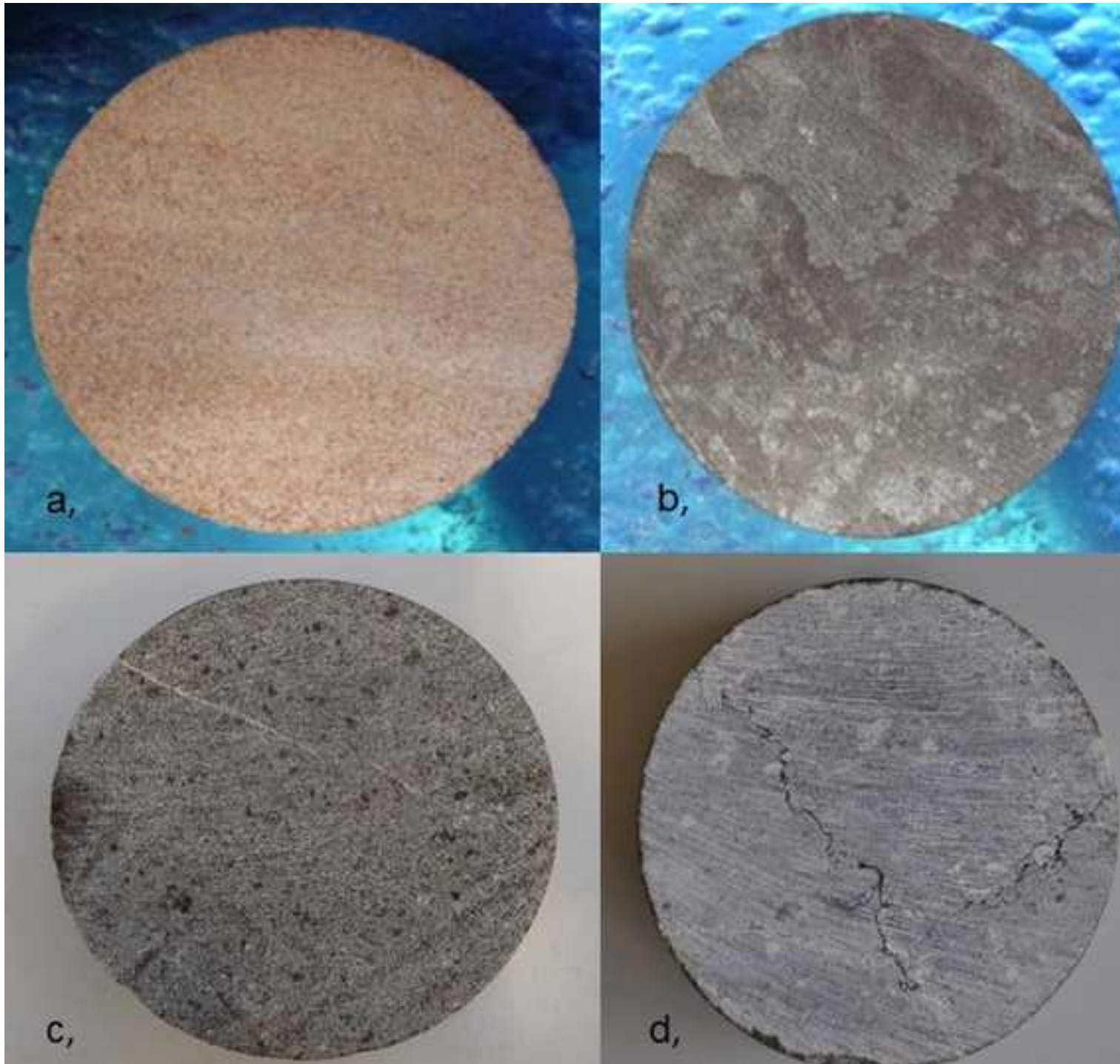
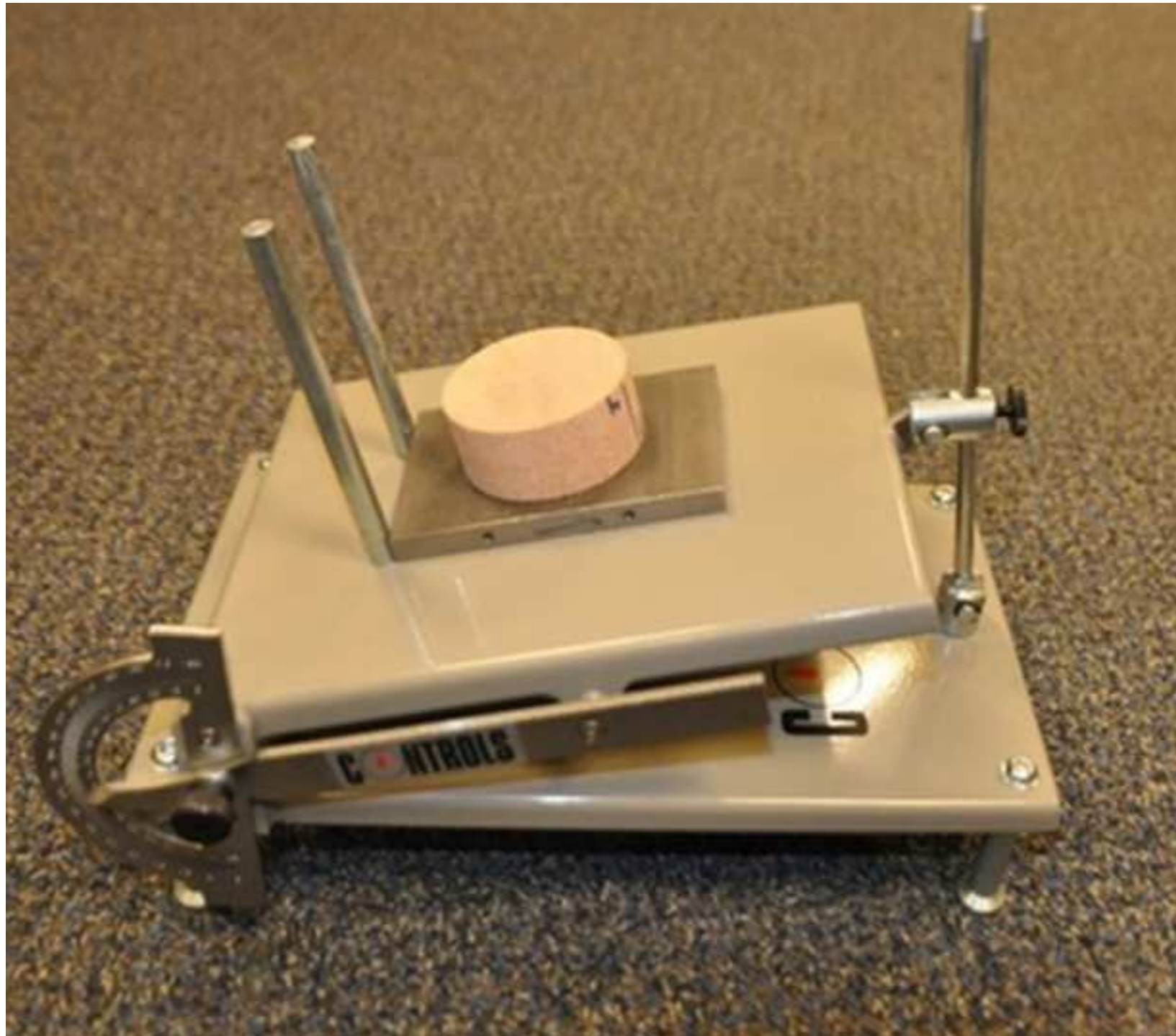


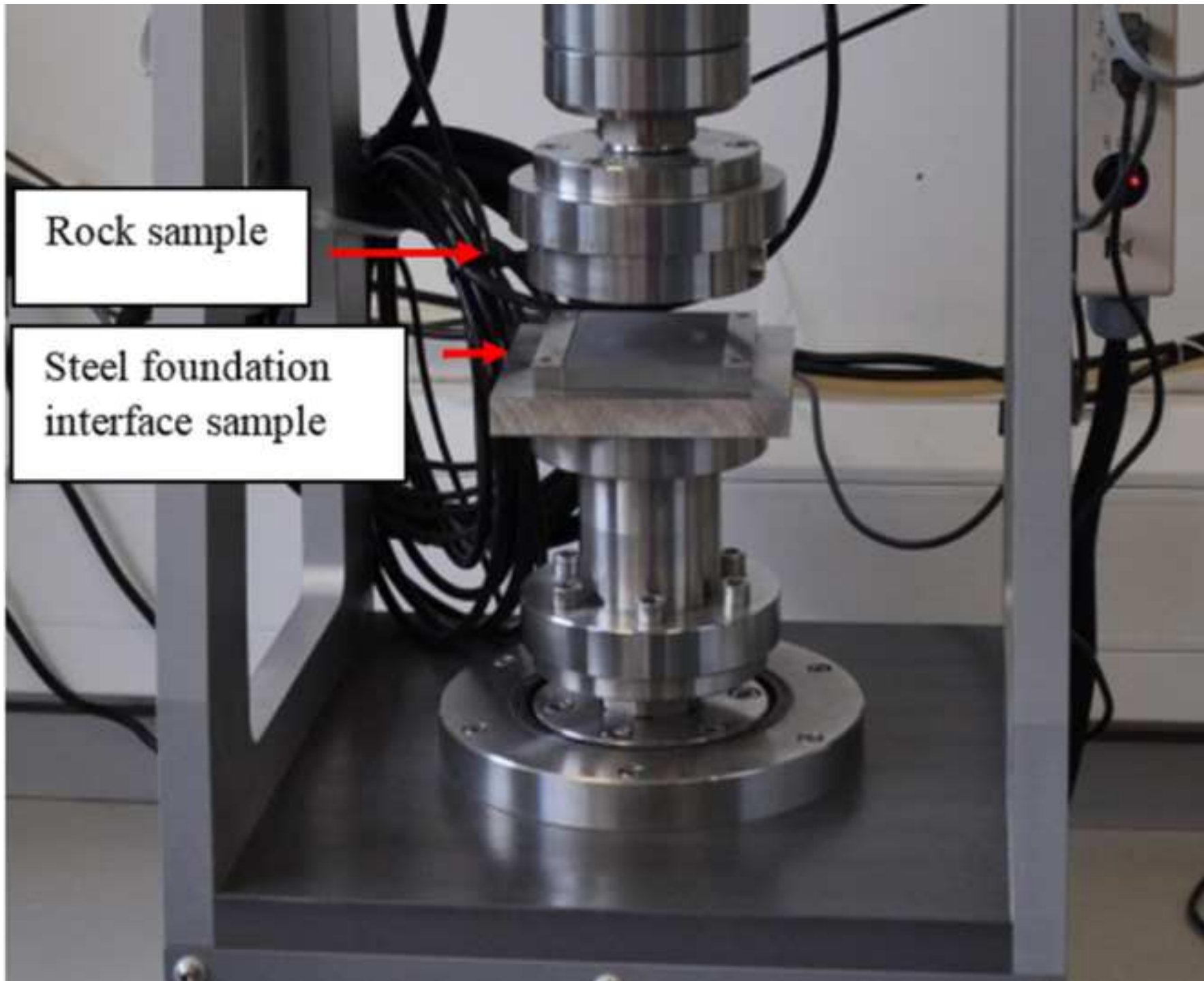
Figure 2 Image of the tilt table testing showing a sandstone sample on a steel interface during interface friction angle determination.

[Click here to access/download;Figure;Figure 2.jpg](#)









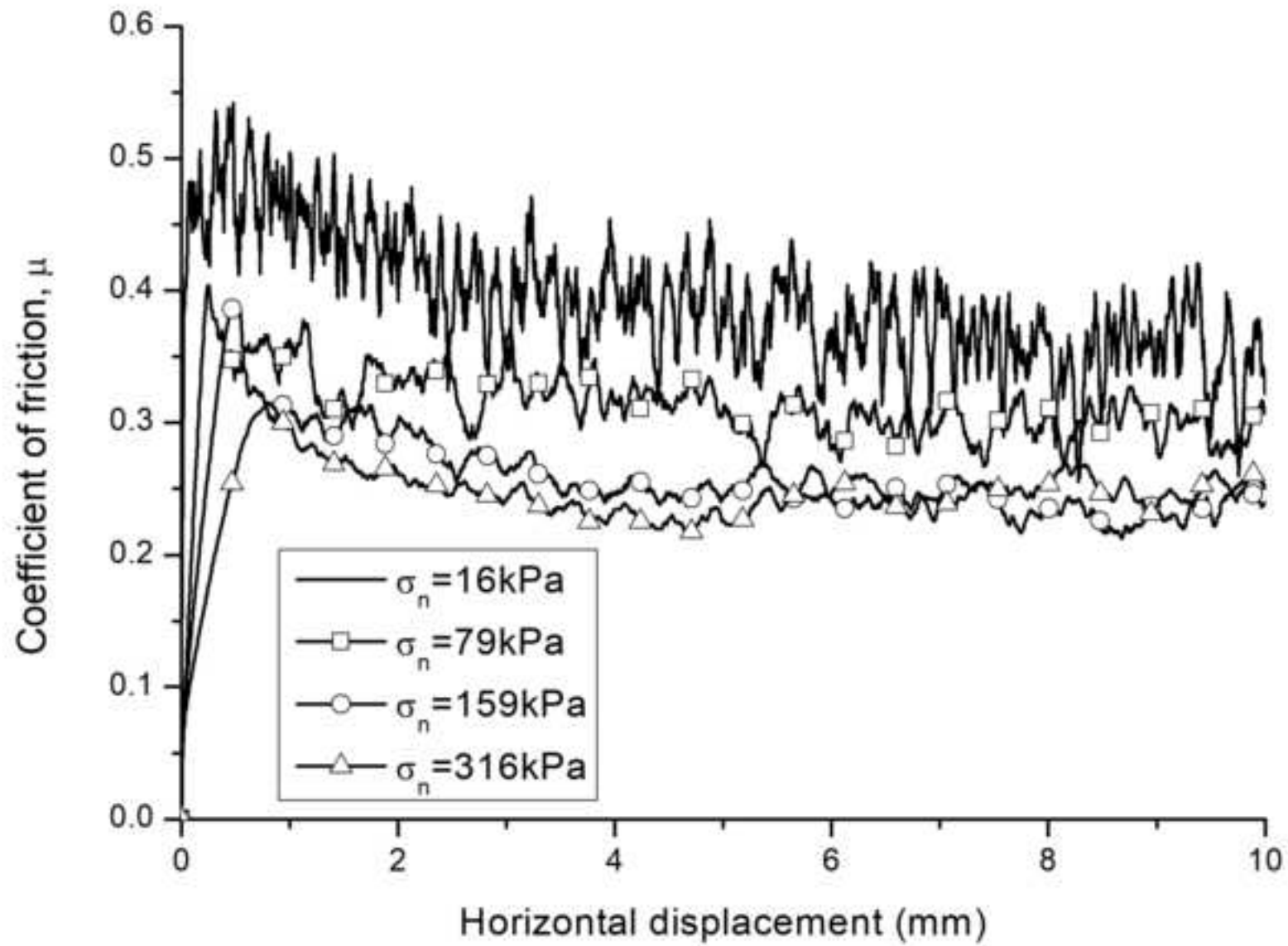


Figure 5 Comparison of peak interface shear resistance for the different rock types tested against the smoothest steel interface at varying stress levels (steel interface Ra

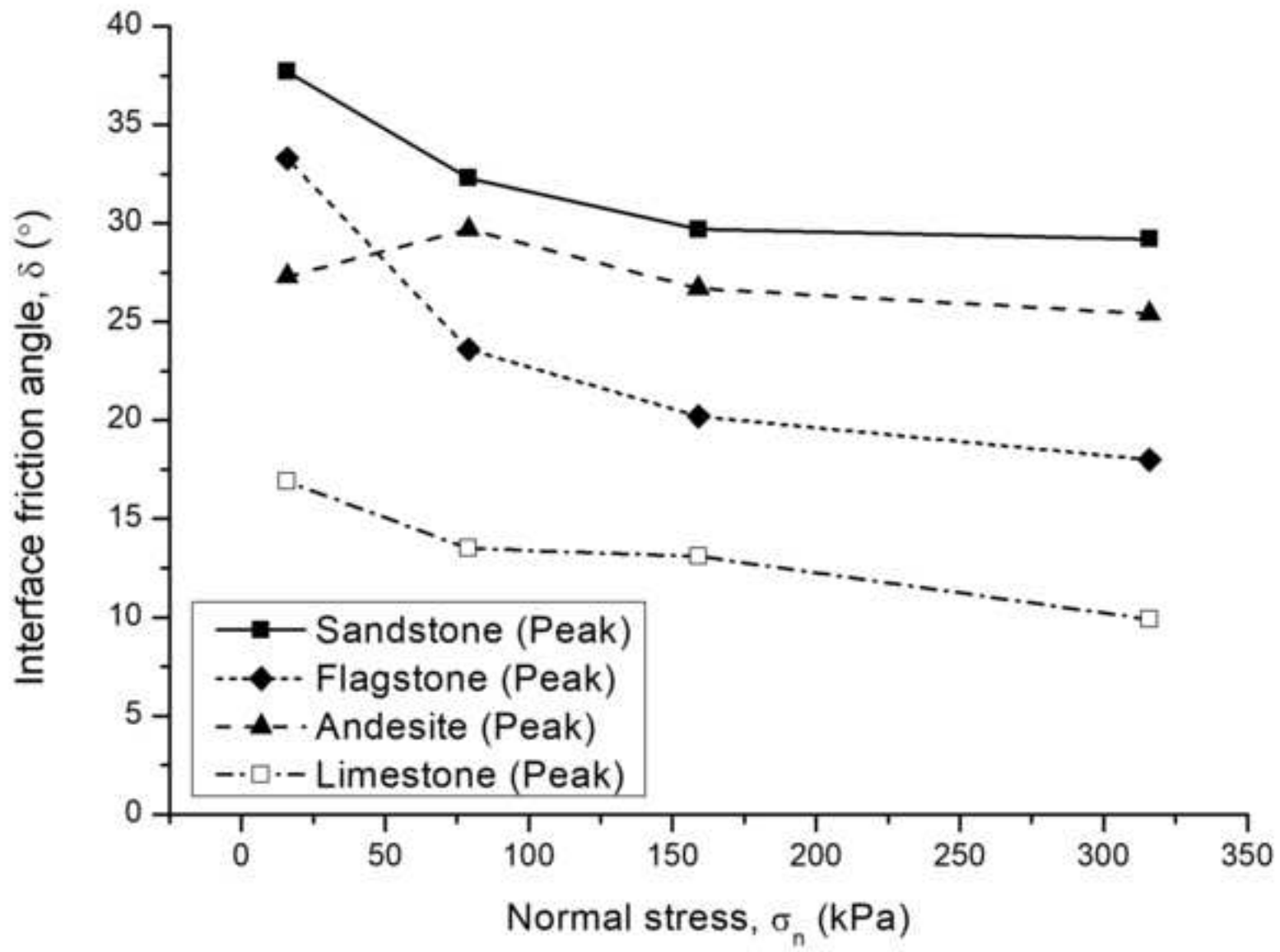


Figure 6a Variation of peak and ultimate interface friction angles with normal stress for the rock types showing comparison of IST testing with results of tilt table tests a)

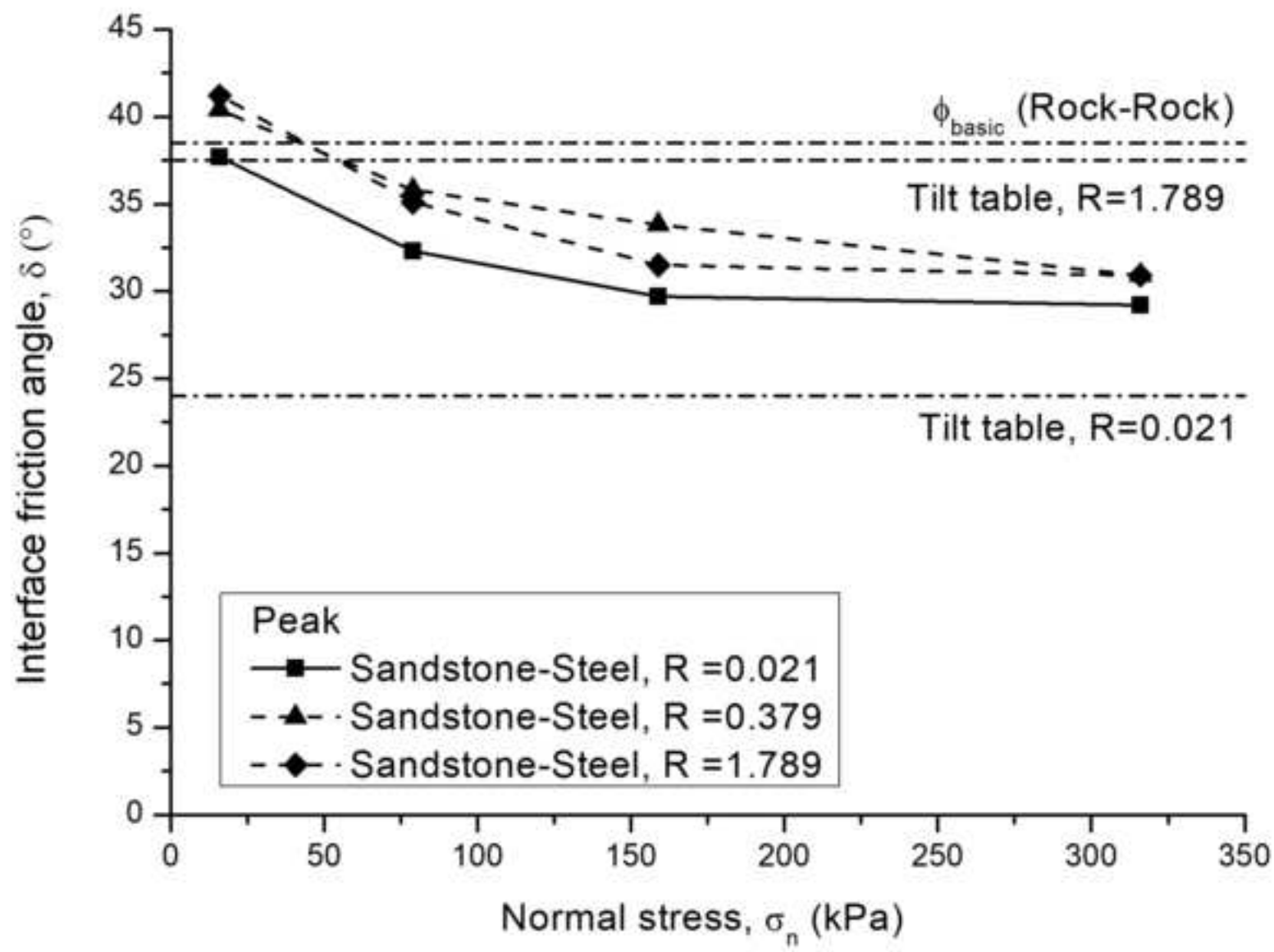


Figure 6b Variation of peak and ultimate interface friction angles with normal stress for the rock types showing comparison of IST testing with results of tilt table tests b)

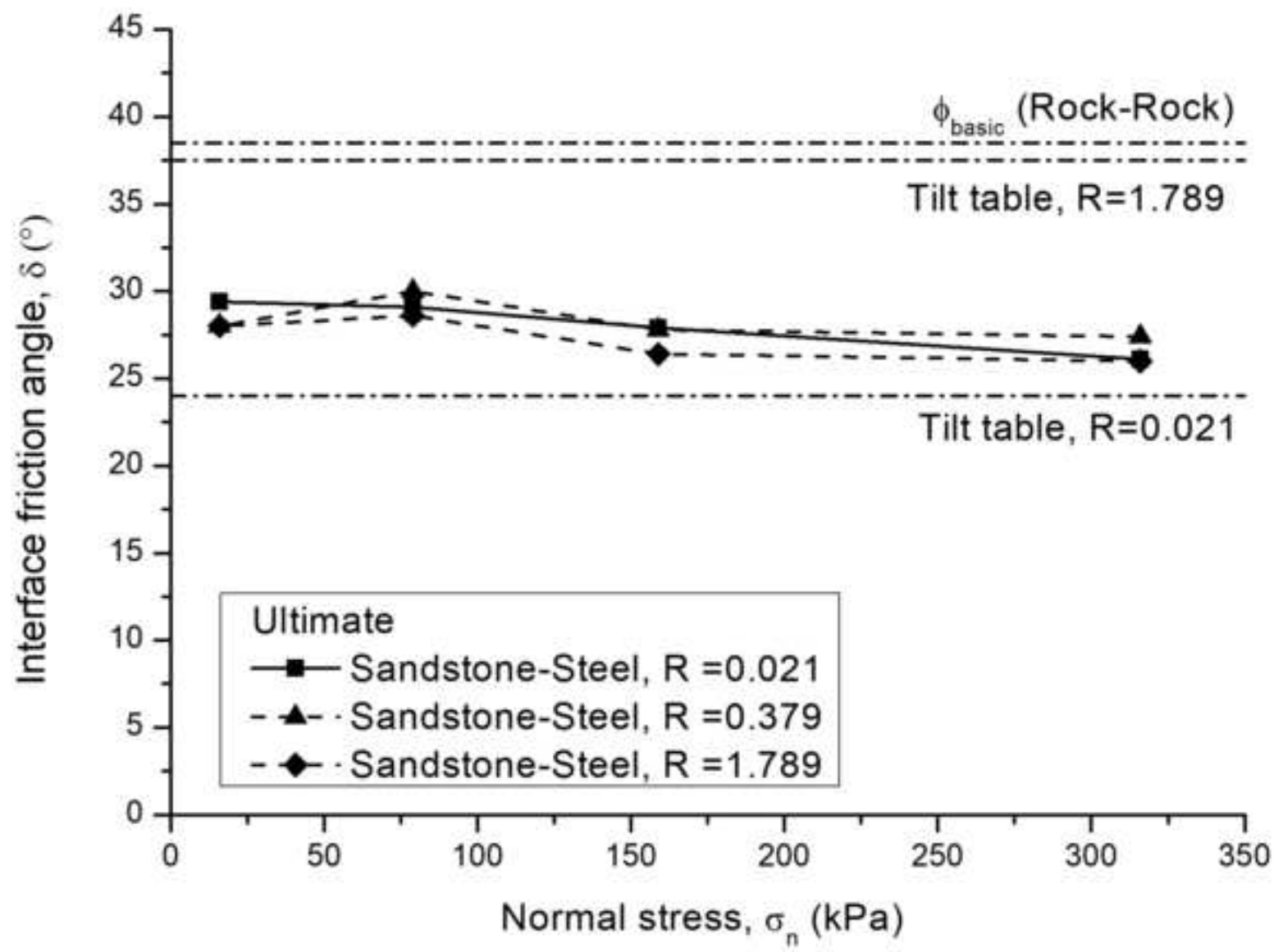


Figure 6c Variation of peak and ultimate interface friction angles with normal stress for the rock types showing comparison of IST testing with results of tilt table tests c)

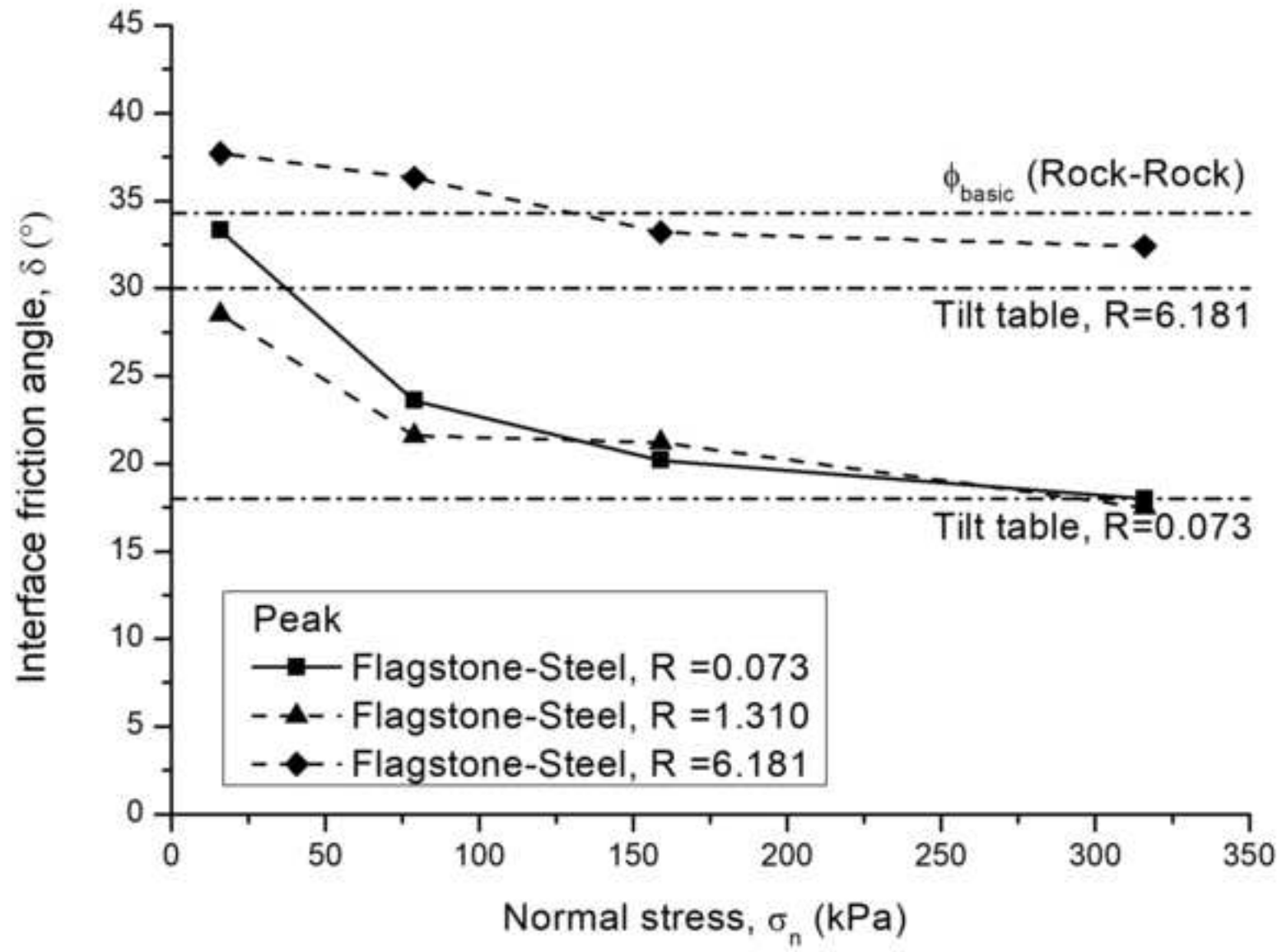


Figure 6d Variation of peak and ultimate interface friction angles with normal stress for the rock types showing comparison of IST testing with results of tilt table tests d)

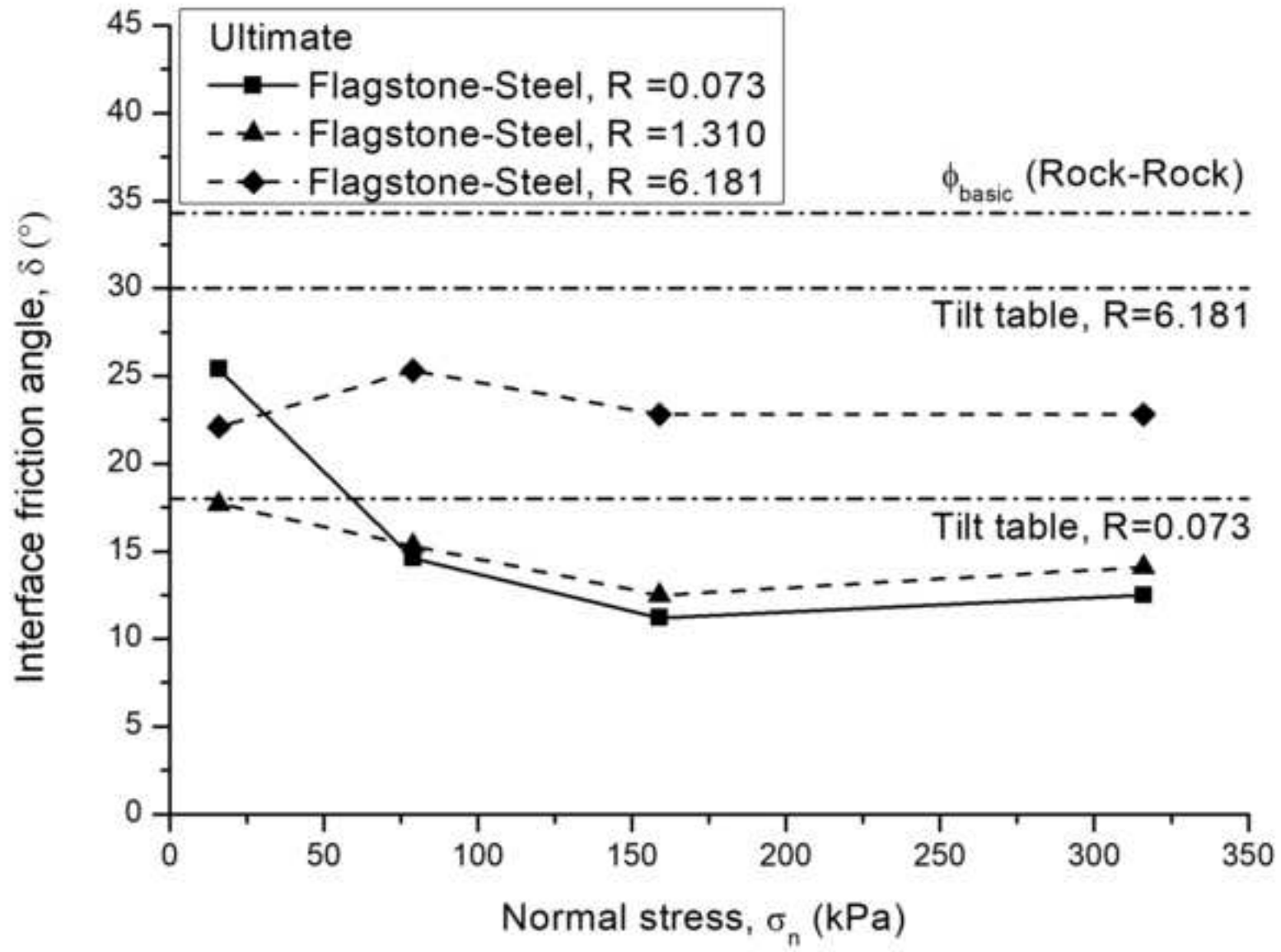


Figure 6e Variation of peak and ultimate interface friction angles with normal stress for the rock types showing comparison of IST testing with results of tilt table tests e)

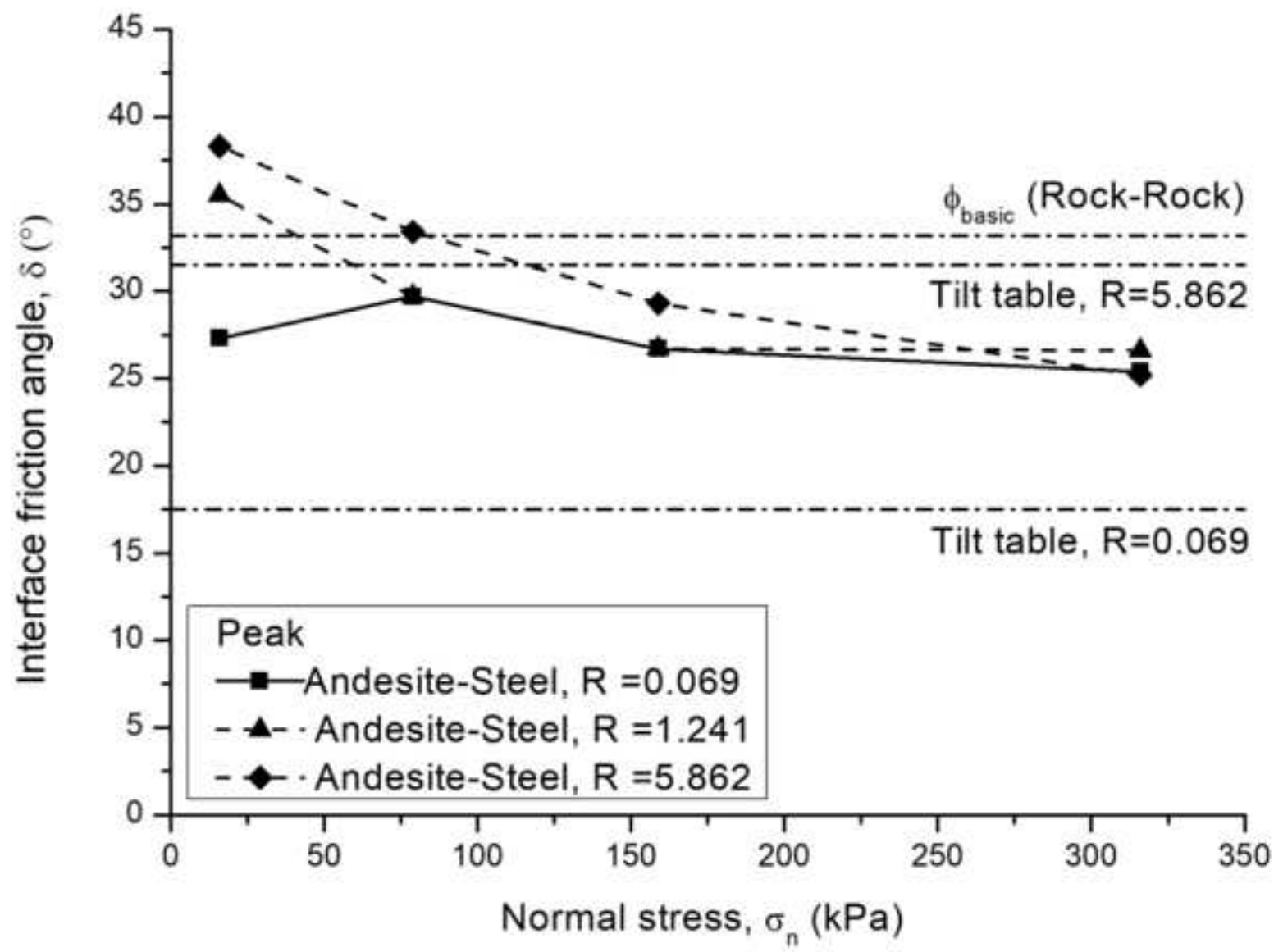




Figure 6f Variation of peak and ultimate interface friction angles with normal stress for the rock types showing comparison of IST testing with results of tilt table tests f)

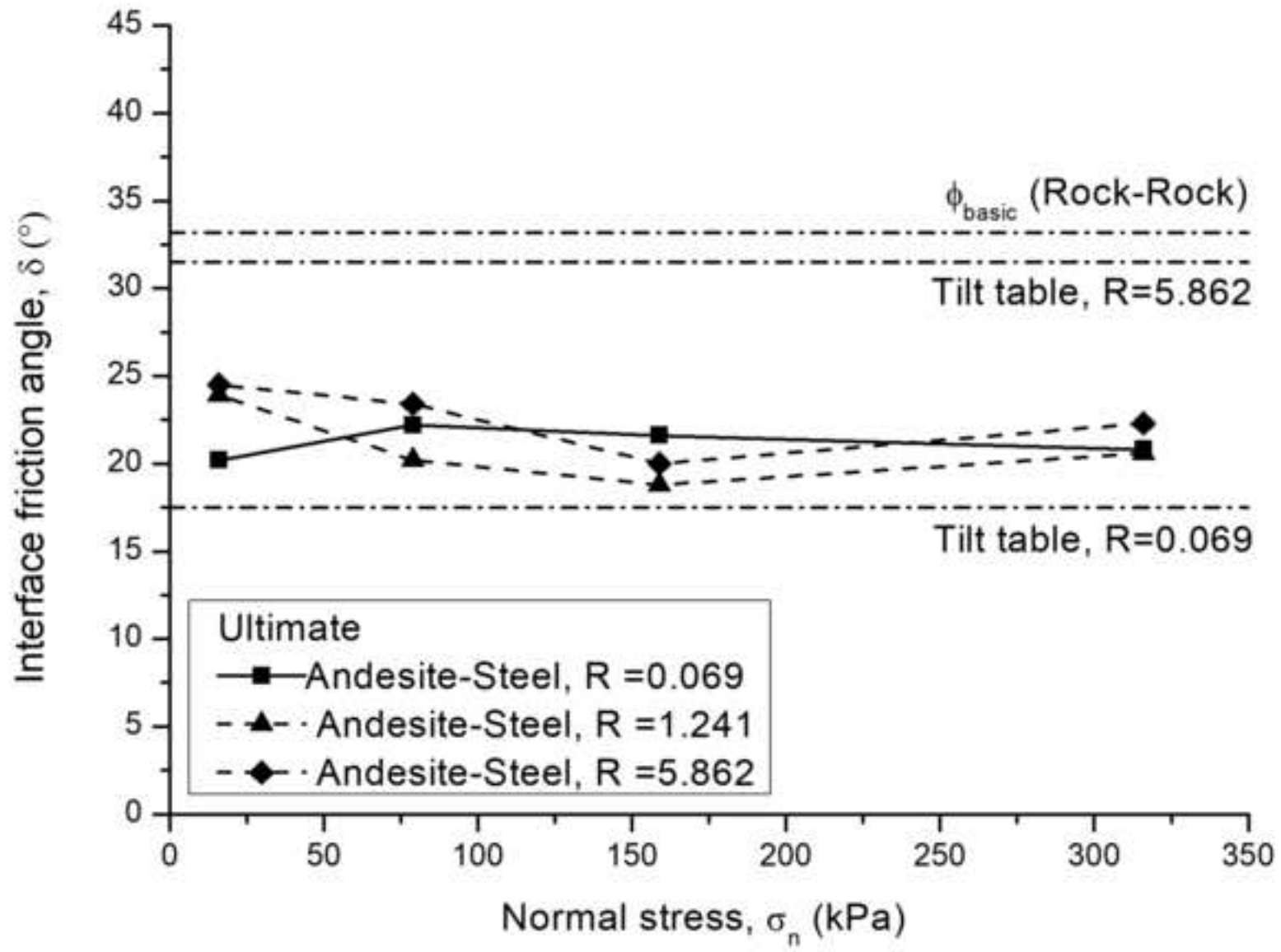


Figure 6g Variation of peak and ultimate interface friction angles with normal stress for the rock types showing comparison of IST testing with results of tilt table tests g)

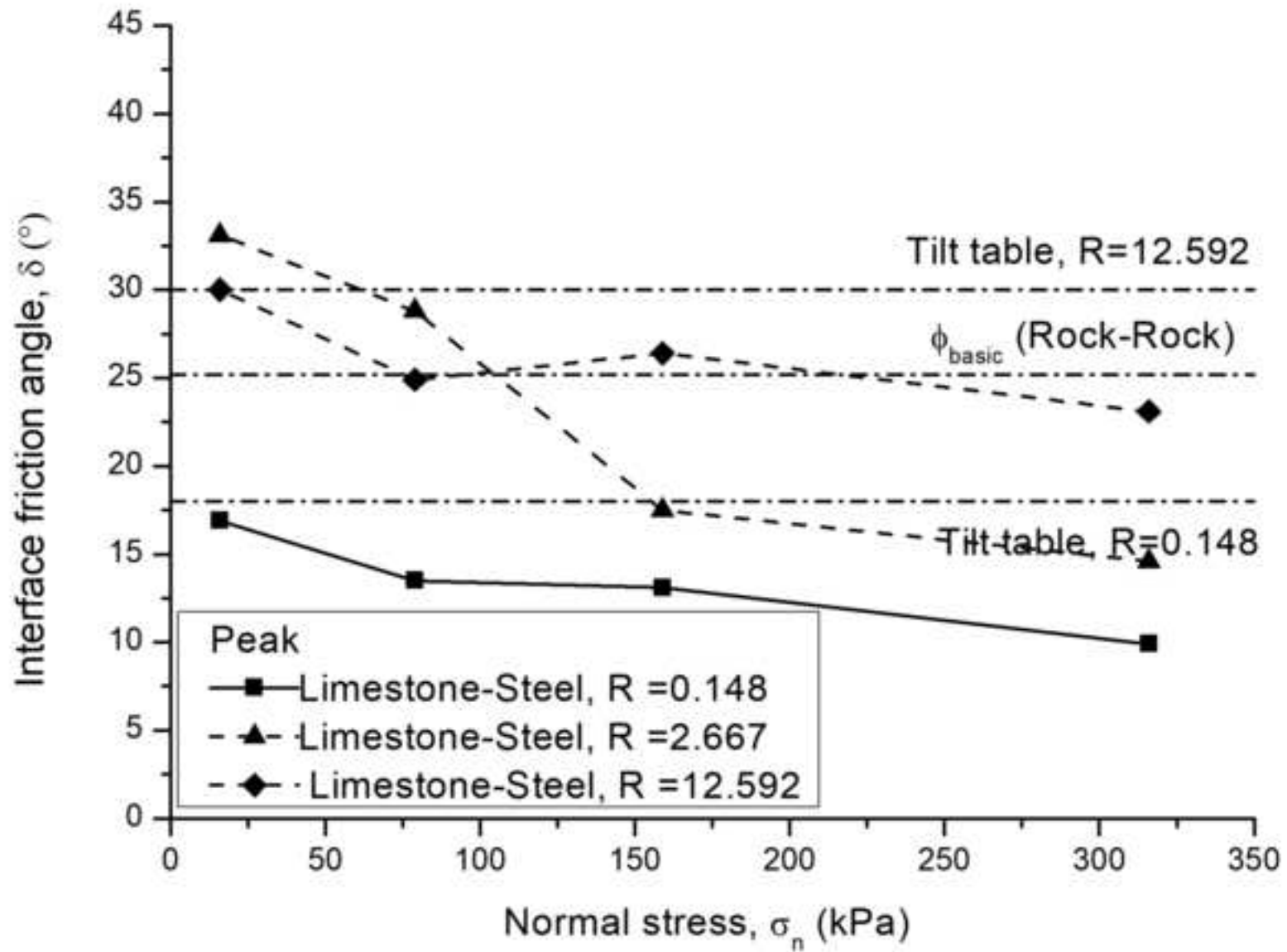


Figure 6h Variation of peak and ultimate interface friction angles with normal stress for the rock types showing comparison of IST testing with results of tilt table tests h)

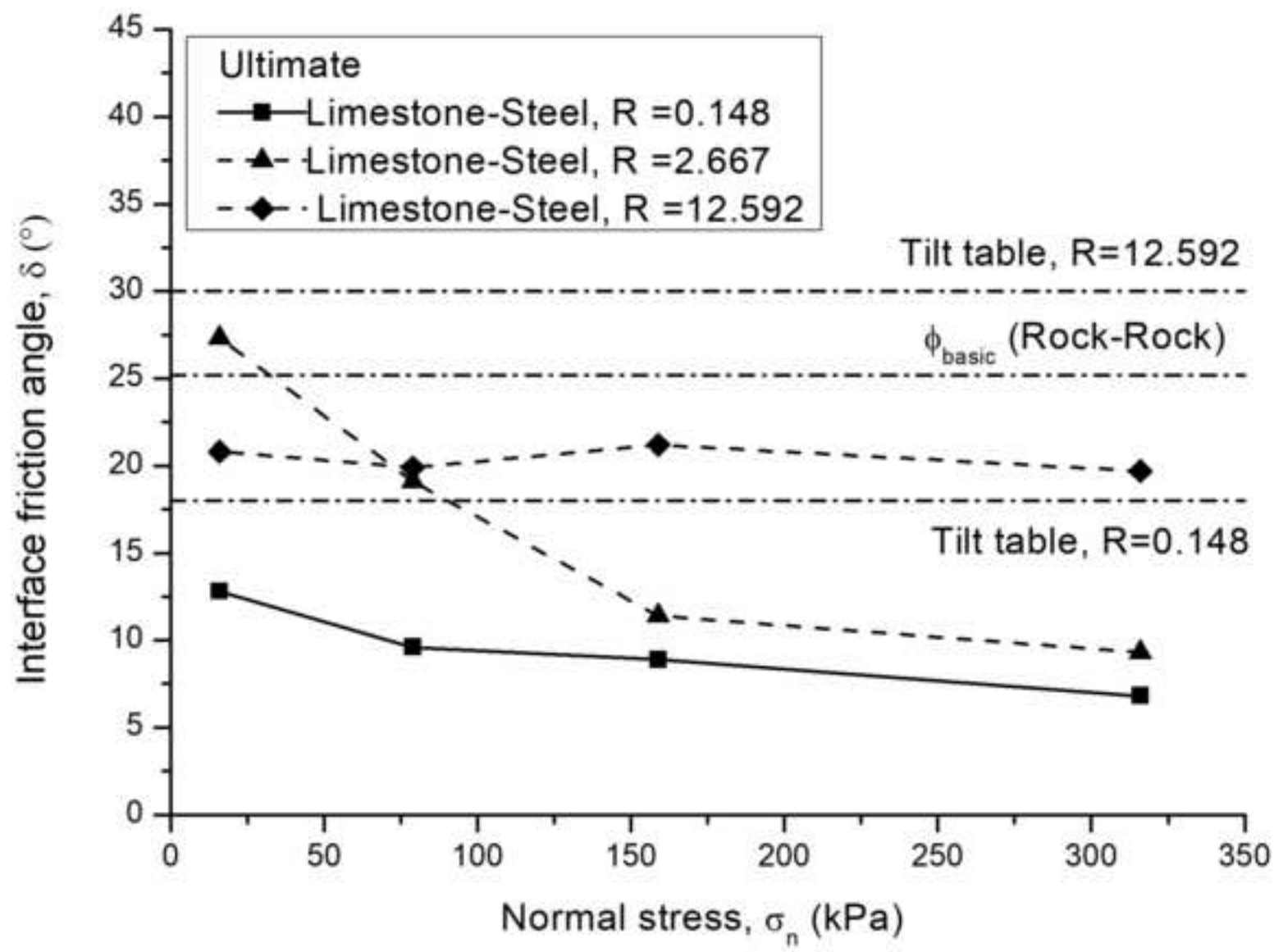


Figure 7a The effect of relative roughness on the average interface friction angles at normal stresses of 159 and 361 kPa a) average peak interface friction angles

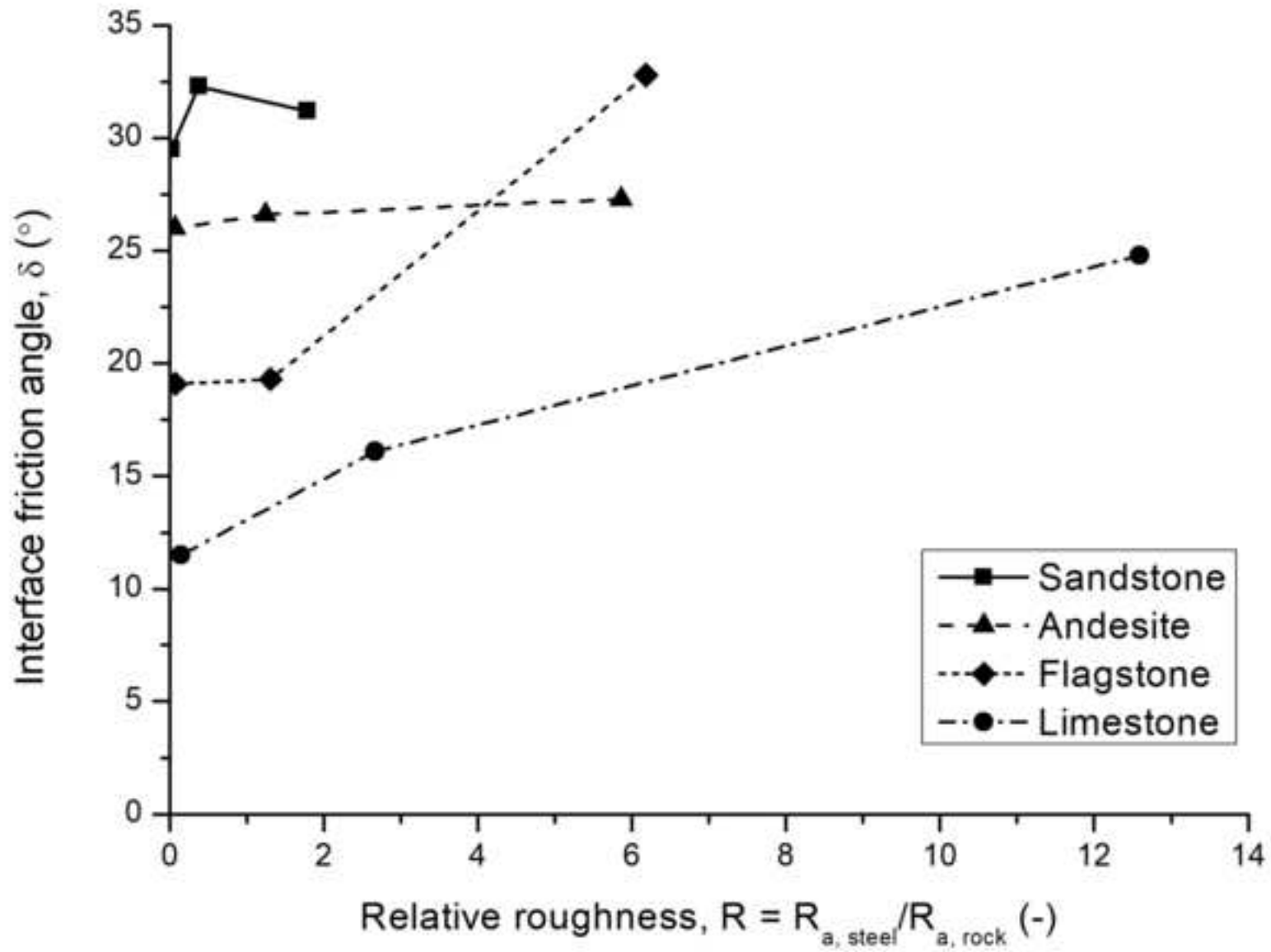


Figure 7b The effect of relative roughness on the average interface friction angles at normal stresses of 159 and 361 kPa b) average ultimate interface friction angles

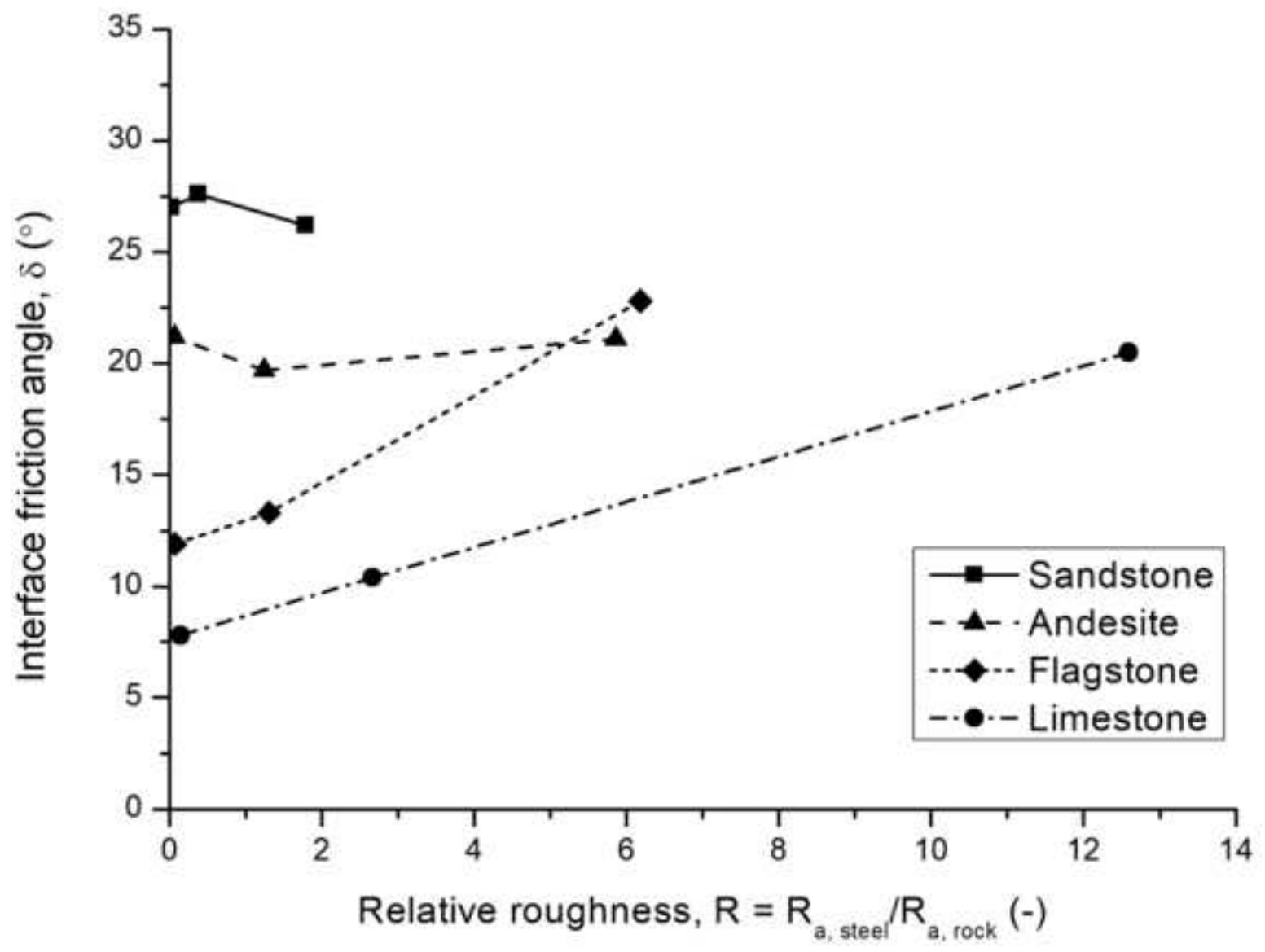


Figure 8a Measurements of normal displacement during interface shear testing a)  
Sandstone and Andesite against steel of  $R_a = 0.4$  and  $34\mu\text{m}$

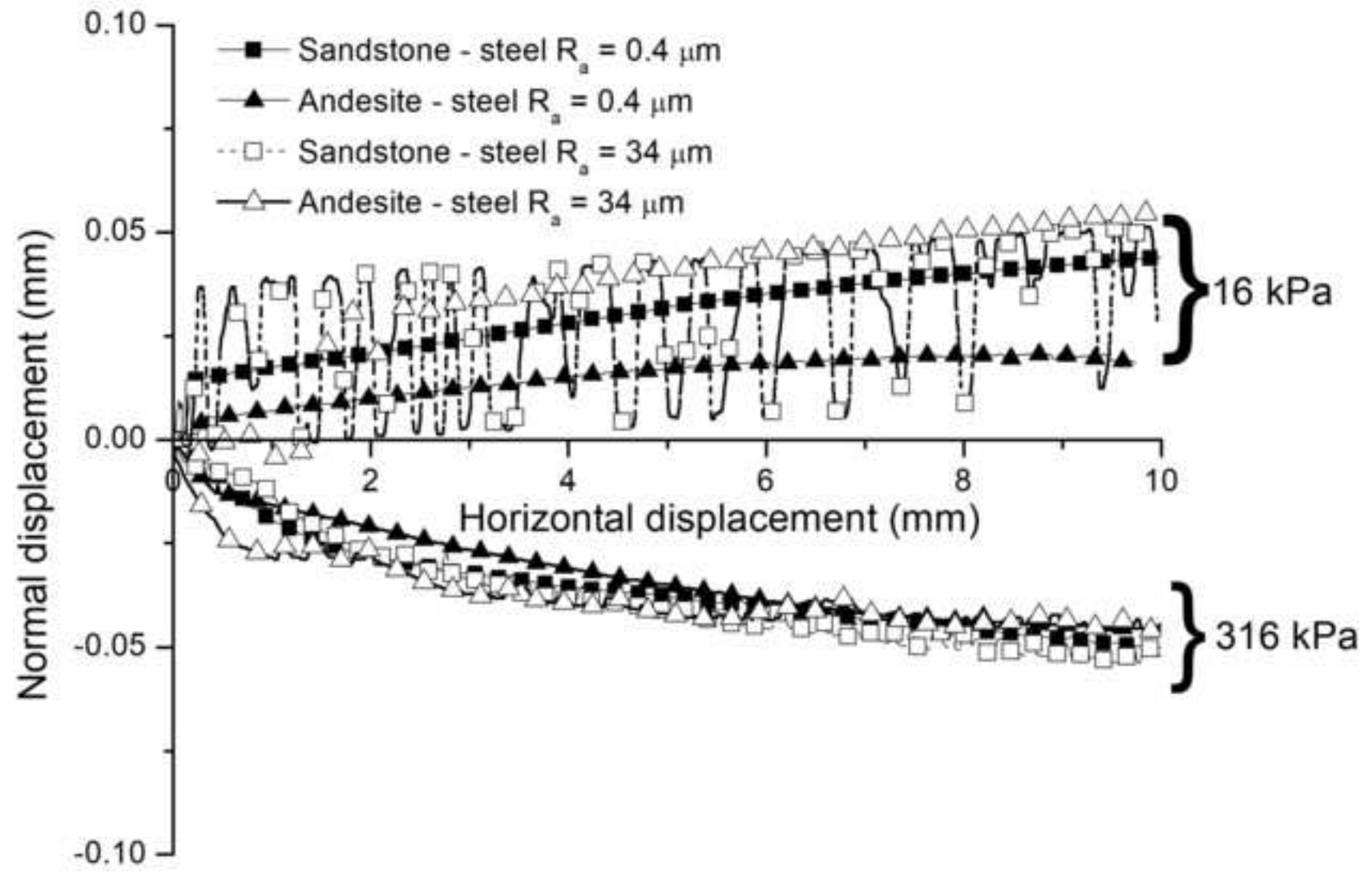
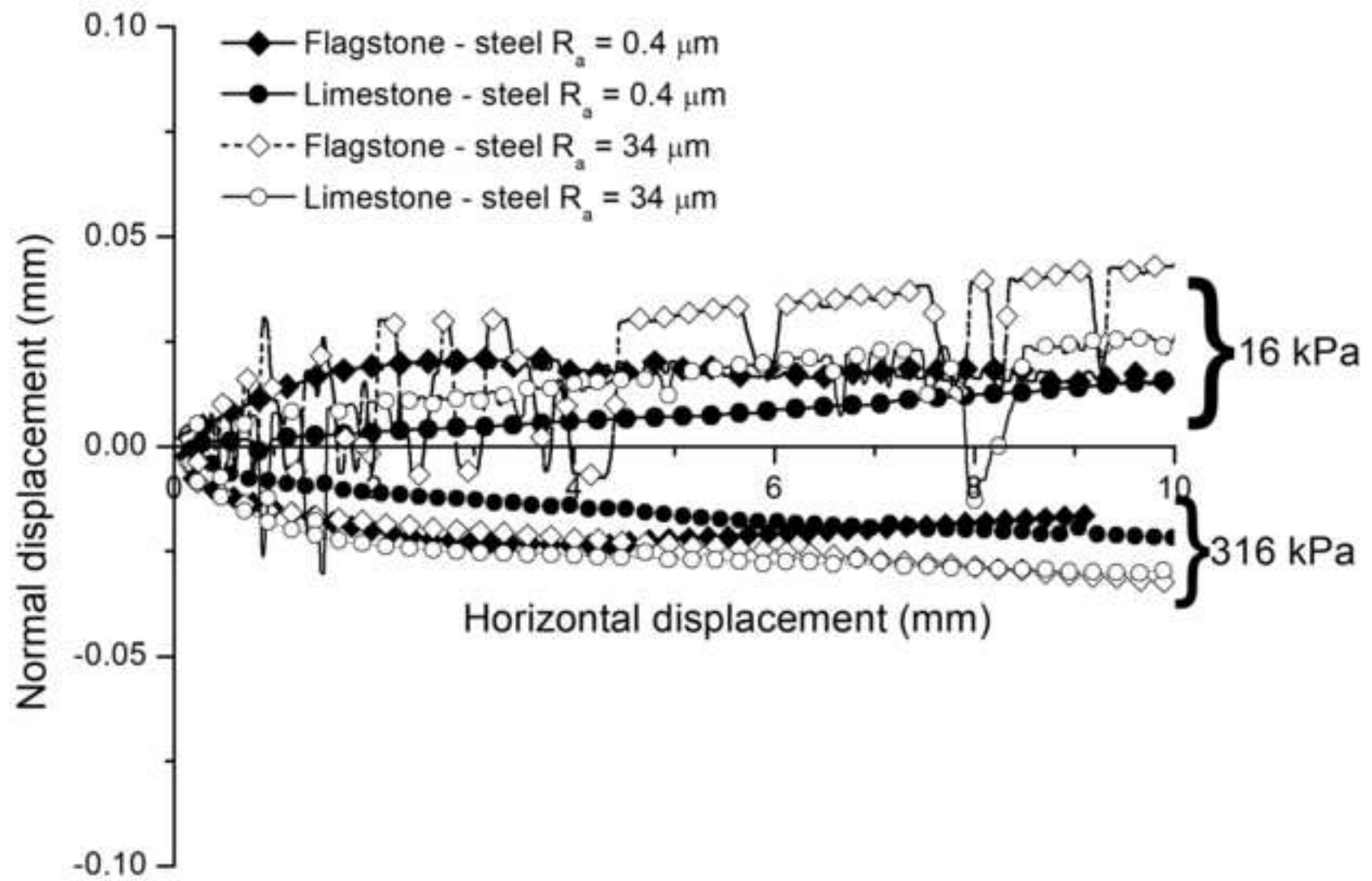


Figure 8b Measurements of normal displacement during interface shear testing b)  
Flagstone and Limestone against steel of  $R_a = 0.4$  and  $34\mu\text{m}$



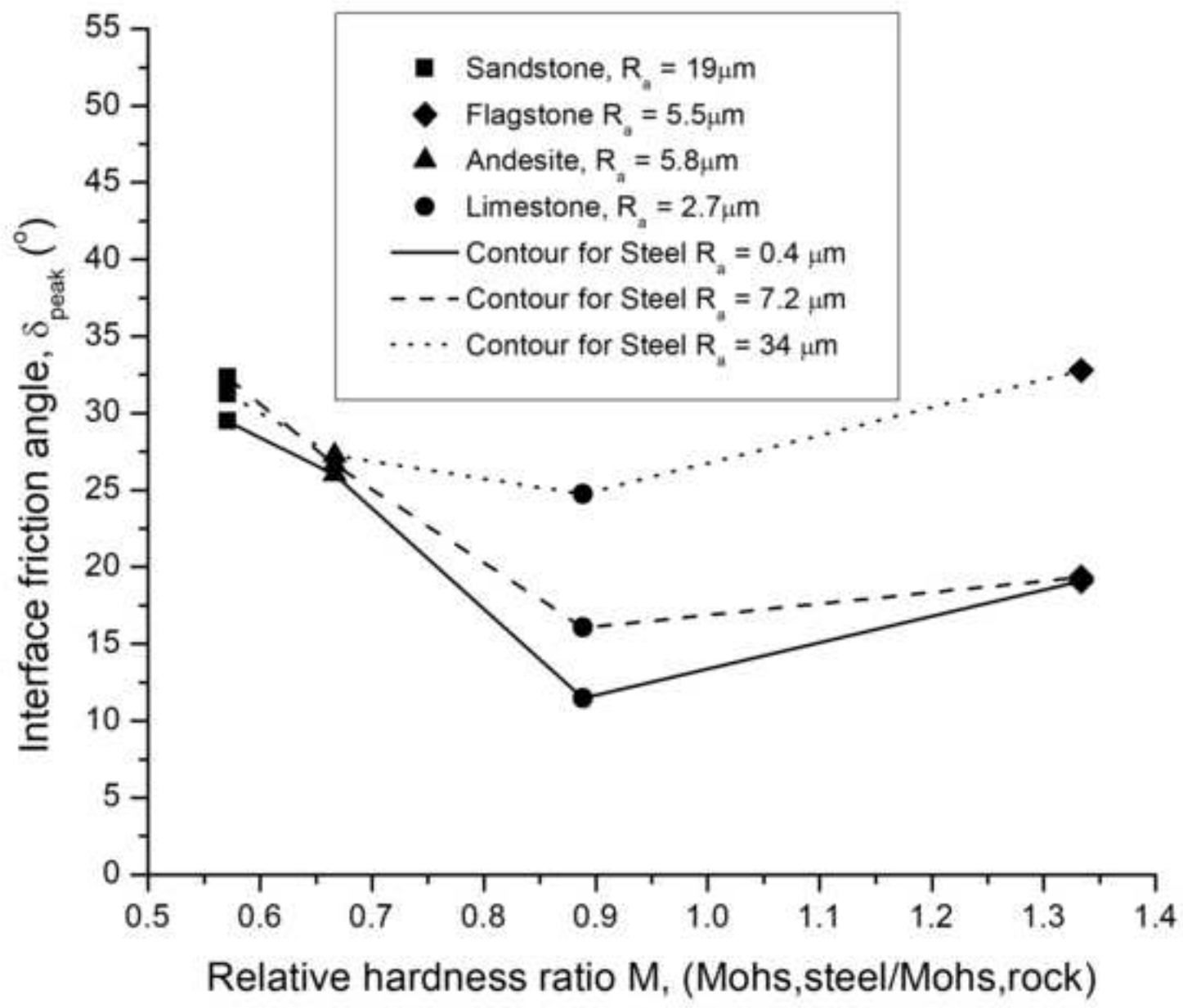




Figure 9b Effect of relative hardness on the interface friction angle b) Average ultimate values of tests at 159 and 316 kPa

[Click here to access/download;Figure;Figure 9b.jpg](#)

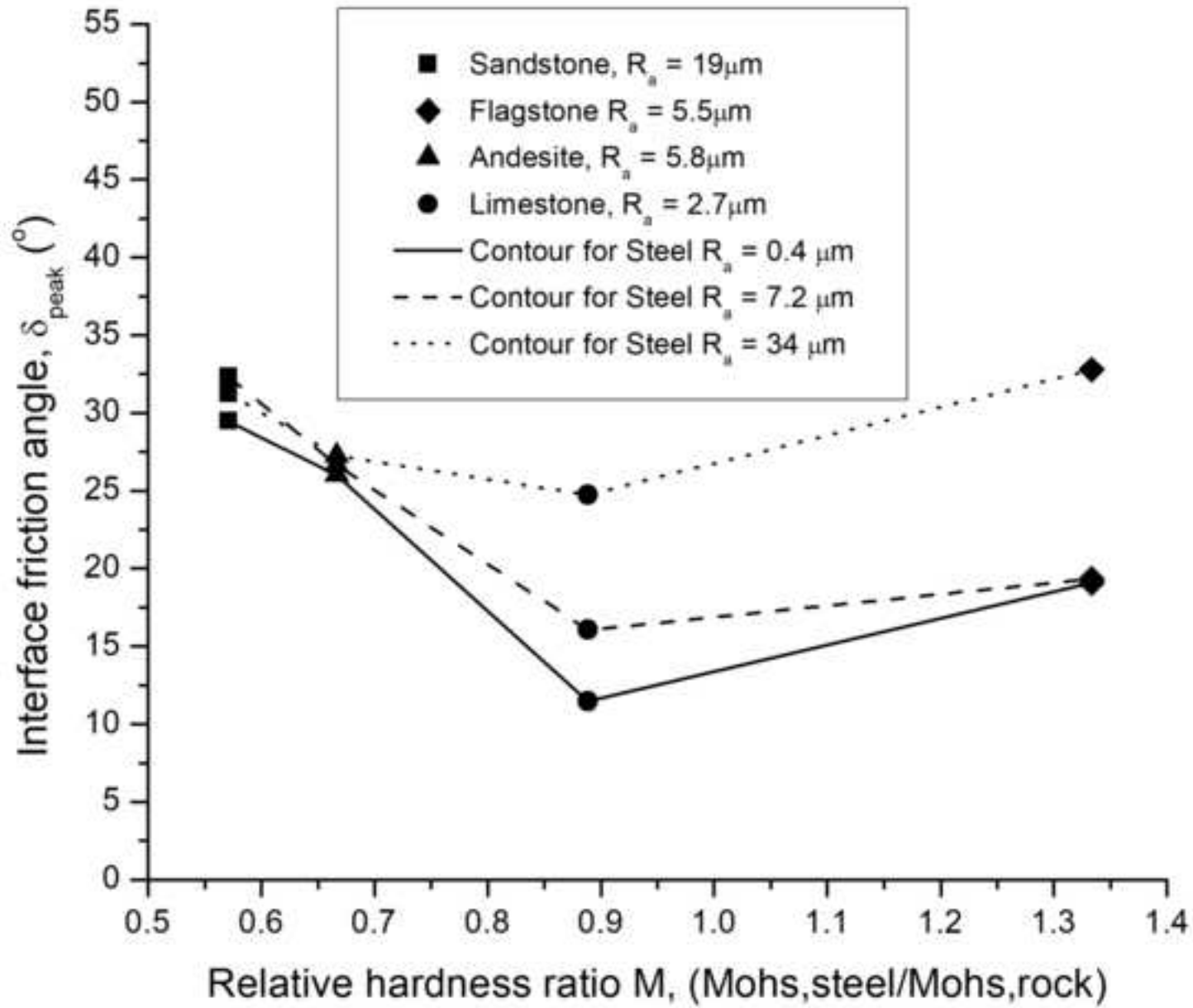


Figure 10 Alpha factor approach for predicting interface shear resistance showing contours for different steel roughness and corresponding arithmetic fitting constants

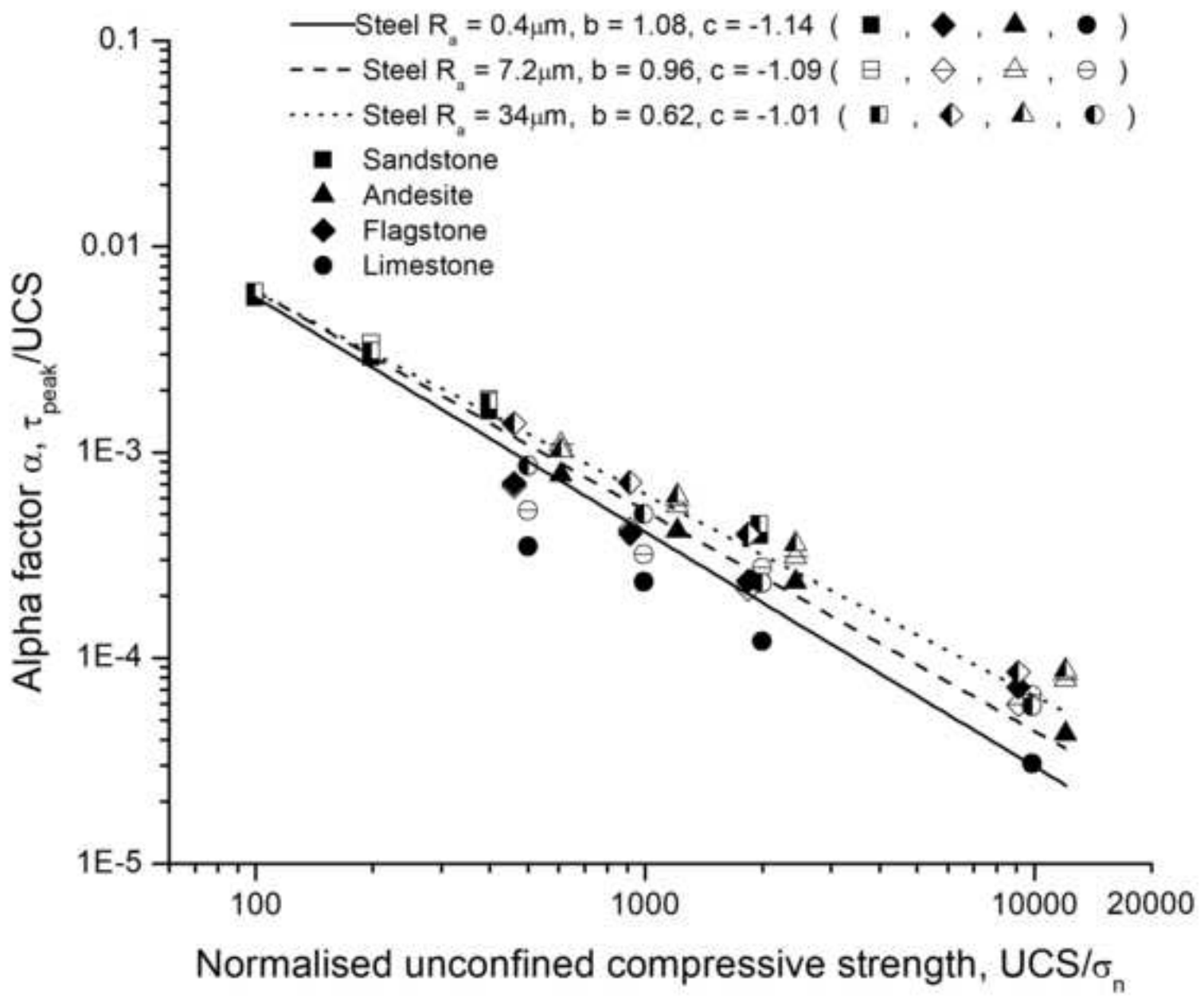


Figure 11 Variation in arithmetic fitting constant b over the range of relative roughness investigated

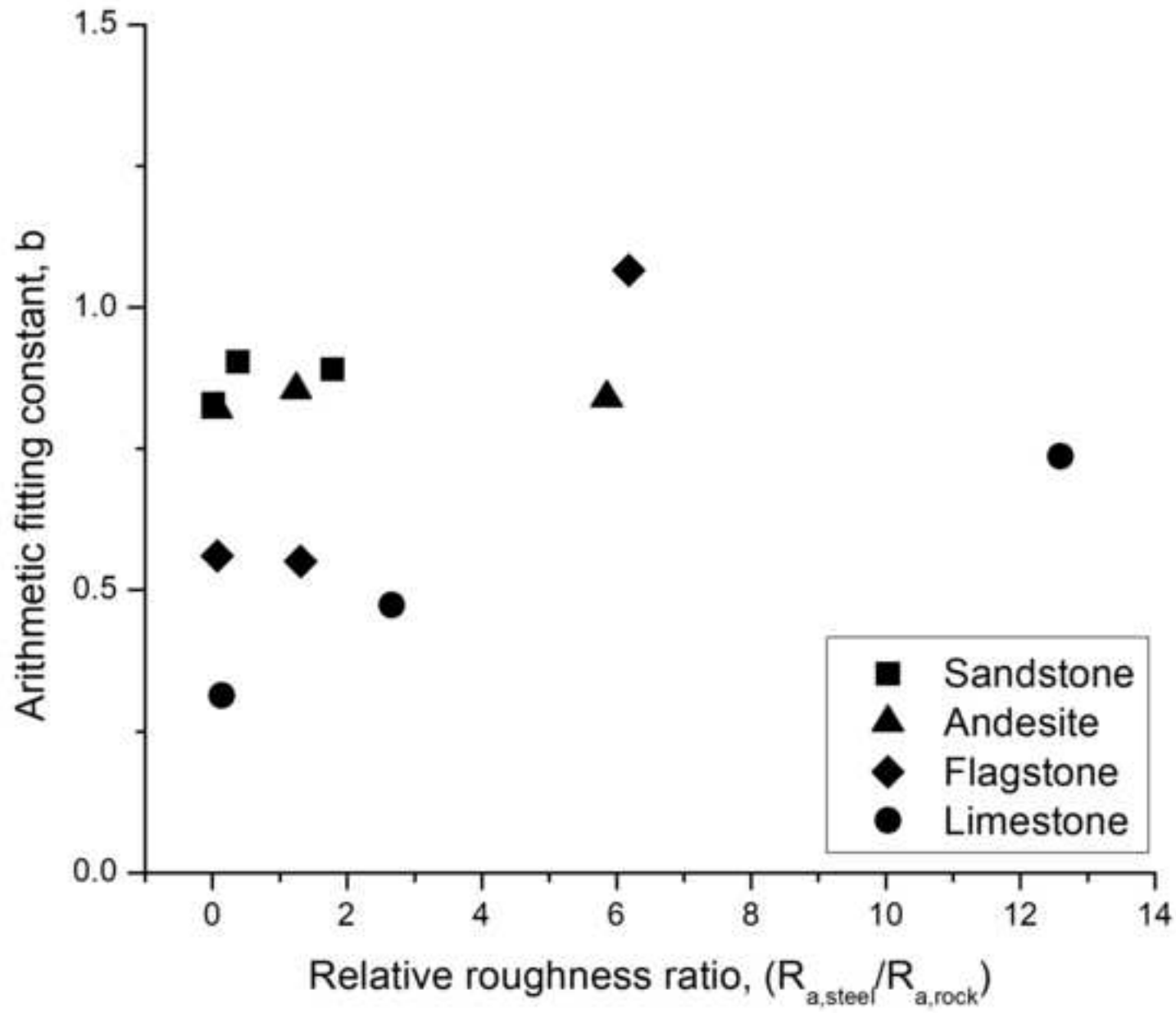


Figure 12a Variation of arithmetic fitting constant over a specific relative roughness range a) Relative roughness range for Sandstone and Andesite interfaces

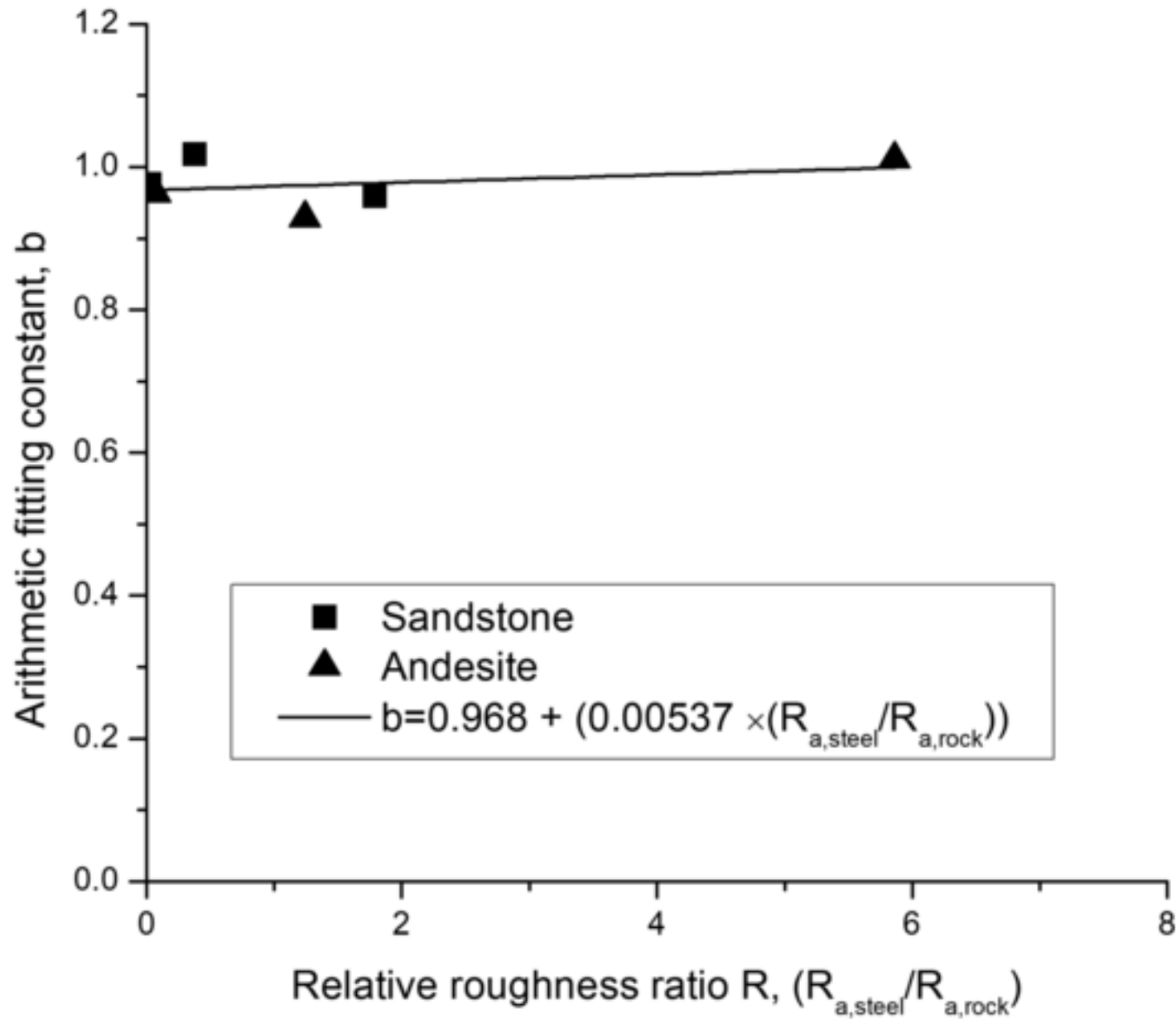


Figure 12b Variation of arithmetic fitting constant bulitmate over a specific relative roughness range b) Relative roughness range for Flagstone and Limestone interfaces

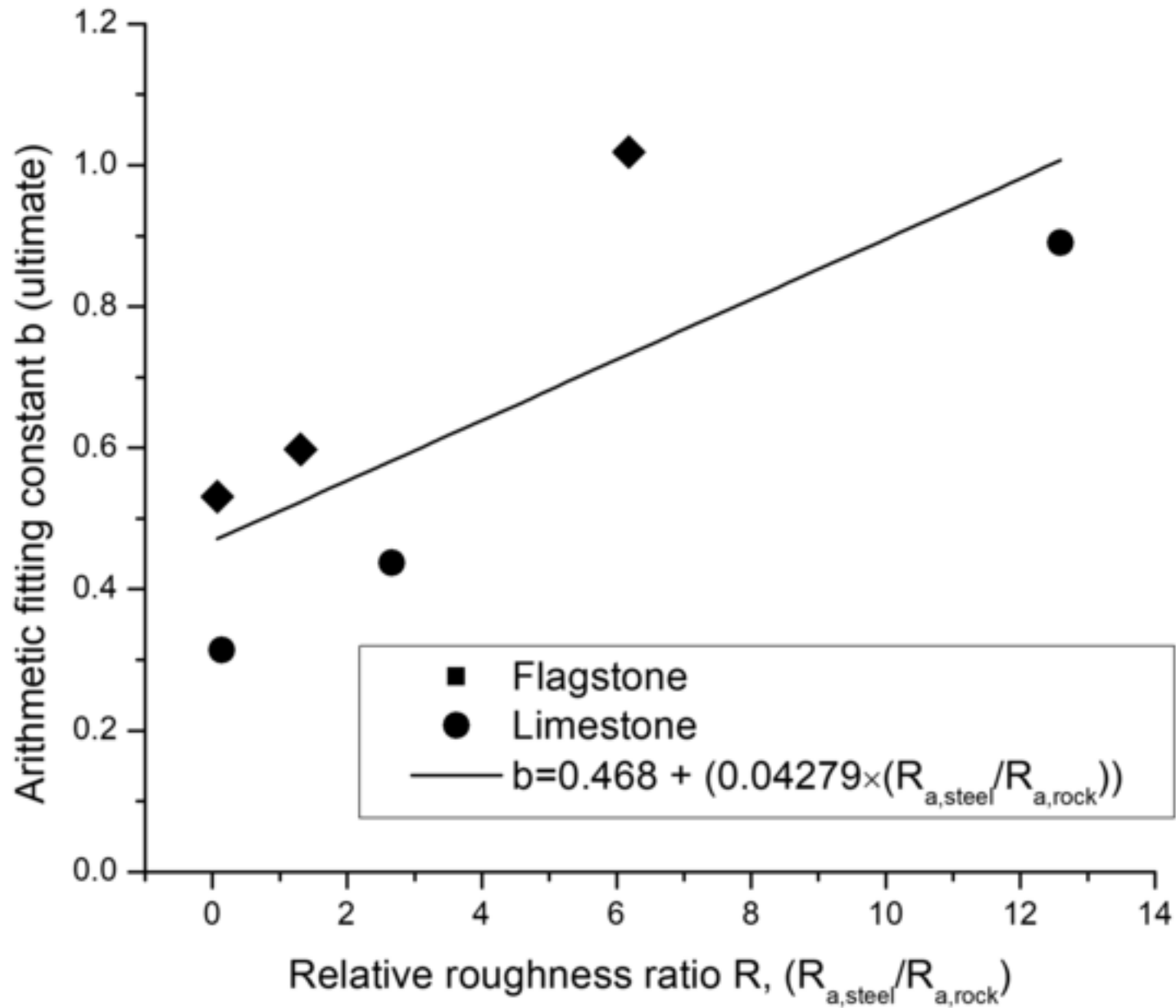


Figure 13a Comparison of measured and calculated interface friction angles a) Test data at all normal stress levels tested (16 to 316 kPa)

[Click here to access/download;Figure;Figure 13a.jpg](#)

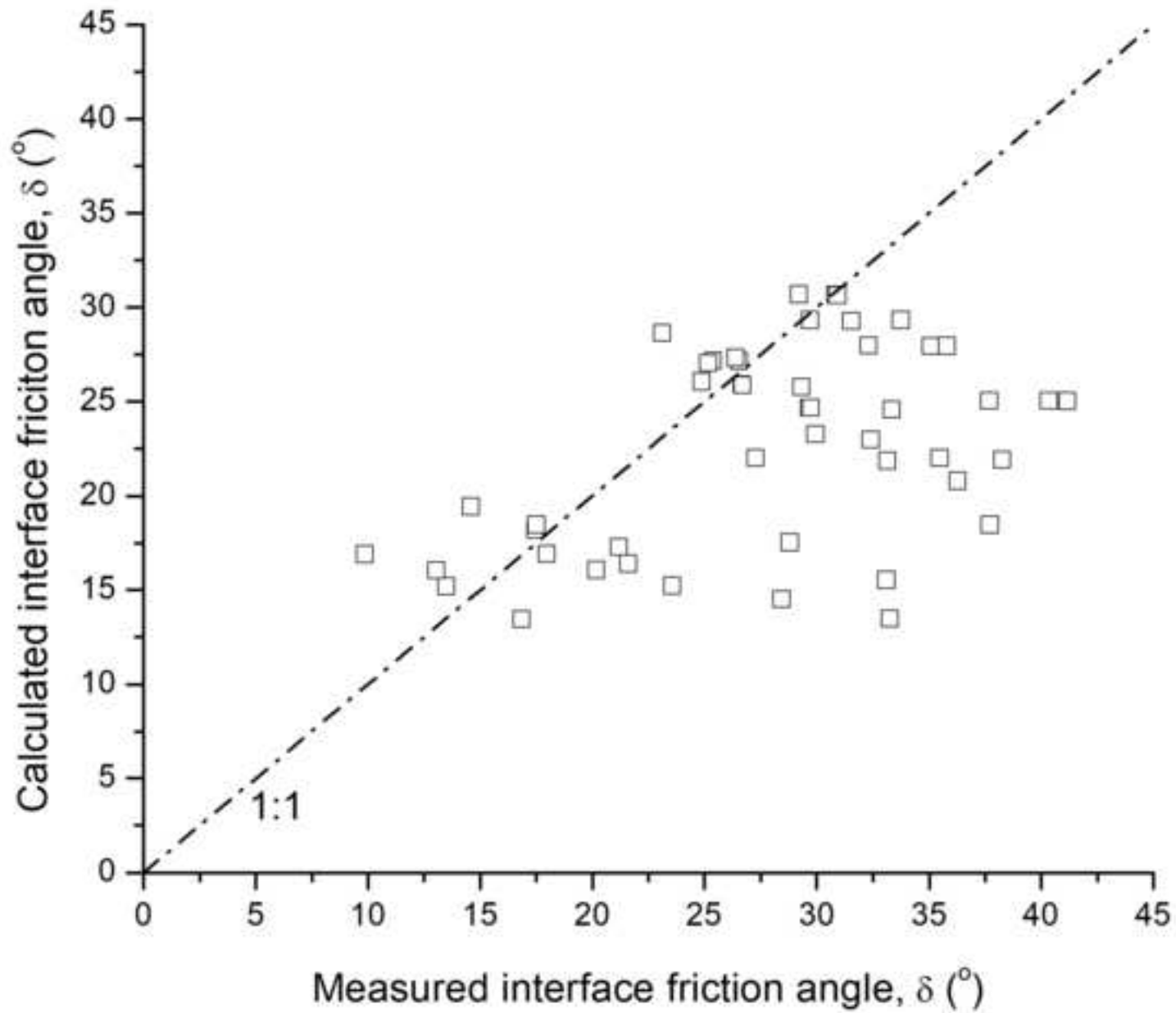


Figure 13b Comparison of measured and calculated interface friction angles b) Test data from tests at normal stresses of 159 and 316 kPa

[Click here to access/download;Figure;Figure 13b.jpg](#)

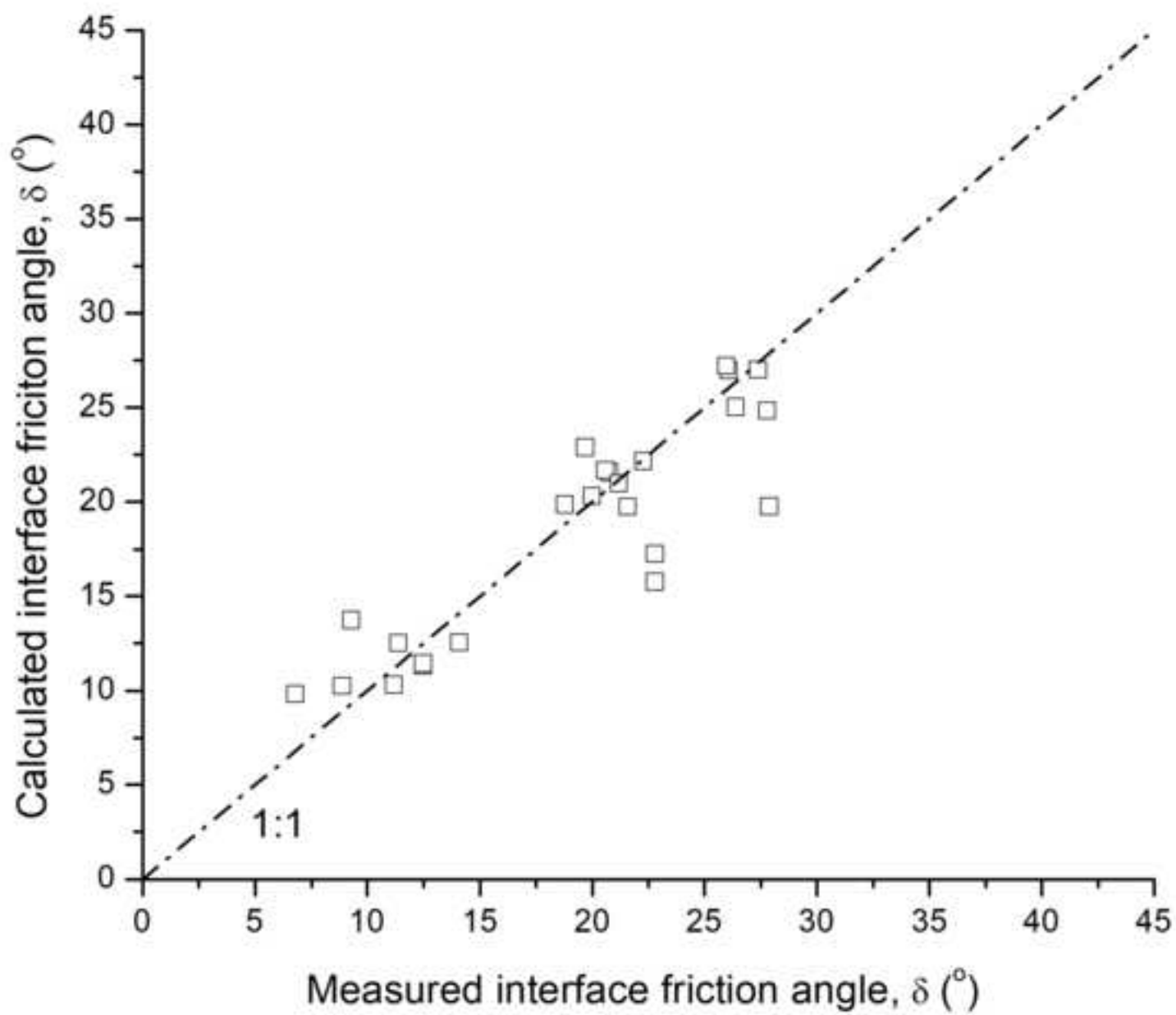


Table 1 Steel interface roughness values compared to those of the rock samples

Steel $R_a$ ( $\mu\text{m}$ )	Relative roughness ratio, R (Equation 5)			
	Sandstone	Flagstone	Andesite	Limestone
0.4	0.021	0.073	0.069	0.148
7.2	0.379	1.310	1.241	2.667
34.0	1.789	6.181	5.862	12.592



Table 2 Summary of the rock characterisation parameters

Rock type	Tensile strength, $T_0$ (MPa)	UCS after Eq. 6 (MPa)	Basic friction angle, $\phi_b$ (°)	Roughness, $R_a$ ( $\mu\text{m}$ )
Sandstone	2.6	34.30	38.5	19
Flagstone	10.0	145.15	34.3	5.5
Andesite	13.0	192.75	33.2	5.8
Limestone	10.8	157.95	25.2	2.7

Table 3 Summary of material surface hardness values

Material	Mohs relative hardness	Vickers hardness (kg/mm <sup>2</sup> )	Relative Hardness, M (Equation 7)
Sandstone	7	1161	0.57
Flagstone	3	157	1.33
Andesite	6	817	0.61
Limestone	4.5	432	0.89
Mild Steel	4	315	-

Table 4 Summary of results from rock – steel interface testing

Rock type	Normal stress (kPa)	R <sub>a</sub> (μm)					
		0.4		7.2		34.0	
		Peak friction angle (°)	Ultimate friction angle (°)	Peak friction angle (°)	Ultimate friction angle (°)	Peak friction angle (°)	Ultimate friction angle (°)
Sandstone	16	37.7	29.4	40.4	28.0	41.2	28.0
	79	32.3	29.1	35.8	30.0	35.1	28.6
	159	29.7	27.9	33.8	27.8	31.5	26.4
	316	29.2	26.1	30.9	27.4	30.9	26.0
Flagstone	16	33.3	25.4	28.5	17.7	37.7	22.1
	79	23.6	14.6	21.6	15.3	36.3	25.3
	159	20.2	11.2	21.2	12.5	33.2	22.8
	316	18.00	12.5	17.5	14.1	32.4	22.8
Andesite	16	27.3	20.2	35.5	23.9	38.3	24.5
	79	29.7	22.2	29.7	20.2	33.4	23.4
	159	26.7	21.6	26.7	18.8	29.3	20.0
	316	25.4	20.8	26.6	20.6	25.2	22.3
Limestone	16	16.9	12.8	33.1	27.3	30.0	20.8
	79	13.5	9.6	28.8	19.1	24.9	19.9
	159	13.1	8.9	17.5	11.4	26.4	21.2
	316	9.9	6.8	14.6	9.3	23.1	19.7

Table 5 Summary of the arithmetic fitting constants b and c in Equation 1

Steel roughness, $R_a$ ( $\mu\text{m}$ )	Peak		Ultimate	
	b	c	b	c
0.4	1.08	-1.14	1.14	-1.18
7.2	0.96	-1.09	1.25	-1.19
34.0	0.62	-1.01	0.62	-1.05

Author photograph







